Report No. 66-9

STRUCTURES AND MATERIALS RESEARCH
DEPARTMENT OF CIVIL ENGINEERING

A STUDY OF A MULTIPLE INTEGRAL REPRESENTATION OF THE CONSTITUTIVE EQUATION OF A NONLINEAR VISCOELASTIC SOLID

BY

V. V. NEIS
and
J. L. SACKMAN

July 1966

STRUCTURAL ENGINEERING LABORATORY
UNIVERSITY OF CALIFORNIA
BERKELEY CALIFORNIA

Structures and Materials Research
Department of Civil Engineering
Division of Structural Engineering
and Structural Mechanics

Report Number 66-9

A STUDY OF A MULTIPLE INTEGRAL REPRESENTATION OF THE CONSTITUTIVE EQUATION OF A NONLINEAR VISCOELASTIC SOLID

by

V.V. Neis
Graduate Student in Civil Engineering
University of California at Berkeley

and
J.L. Sackman
Professor of Civil Engineering
University of California at Berkeley

Contract Number DA-31-124-ARO-D-460
DA Project No: 20014501B33G
ARO Project No: 4547-E

Structural Engineering Laboratory
University of California
Berkeley, California

July 1966

ABSTRACT

The applicability of a functional polynomial of third degree for the constitutive equation of a nonlinear viscoelastic polymer has been investigated. A method for the determination of the kernel functions appearing in the one-dimensional creep formulation has been discussed. Creep measurements of tension and compression in low density polyethylene under single step, two step, and three step loading histories are described. The analysis of this data has provided a basis for the determination of the creep kernel functions. For the loading range used in the tests, the Volterra-Fréchet multiple integral expansion of the constitutive functional of low-density polyethylene has been found to be adequately represented by the three term integral representation. A number of cases of general load histories were investigated. A close comparison between the experimental response to these loading histories and the response predicted by the three term integral representation was obtained.

This page is left blank

TABLE OF CONTENTS

NOTATION

$\boldsymbol{\sigma} = \| \sigma_{ij} \|$	Stress tensor
$\mathbf{E} = \| E_{ij} \|$	Finite strain tensor
e_{ij}	Infinitesimal strain tensor
x_i	Rectangular Cartesian coordinates
$\mathbf{c} = \| \frac{\partial x_i}{\partial X_j} \|$	Deformation gradient
$\delta(t)$	Dirac delta function
$H(t)$	Heaviside step function
M	Relaxation functions
J , K	Creep functions
t	Present time
τ_1, τ_2	Generic times

I. INTRODUCTION

For many physical systems or processes the output of the system is dependent only on the present value of the input. In the majority of cases, however, the output of the system depends upon the past history of the input. For example, the temperature at a given instant of time in an electric furnace is not only dependent on the current flowing in the heating element at that instant, but also on the past history of electric current applied. The history dependent system of interest in this investigation is a visco-elastic material which creeps under sustained loading or which relaxes under sustained deformation. Such hereditary systems may be characterized by a functional relating the history of the input to the present value of the output.

During the early part of the Twentieth Century V. Volterra [1]* and M. Fréchet [2] (among others), presented studies on the general theory of functionals. Fréchet in particular demonstrated that every continuous functional can be represented by a sum of multiple integrals. Volterra used this multiple integral representation for functionals and demonstrated how hereditary phenomena in elasticity, electromagnetism, etc., give rise to nonlinear constitutive equations which may be represented as sums of multiple integrals.

*Numbers in square brackets refer to the bibliography at the end of the text.

A rigorous treatment of the three dimensional constitutive equations for nonlinear viscoelastic materials was presented by Green, Rivlin and Spencer [3]. They assumed that the stress tensor was dependent upon the entire past history of displacement gradients, then - using invariance requirements, results from the theory of matrix invariants, and the Weierstrass theorem on approximation of continuous functions by polynomials - these authors were able to show that the constitutive equation for isotropic hereditary materials could be approximated by a multiple integral expansion. The integrands of the various integrals contain matrix products of the strain tensor and invariants of these matrix products.

Spencer and Rivlin [4] extended the theory of matrix polynomials and were able to reduce the number of matrix products and the number of invariants that need to be considered in Green and Rivlin's formulation. A lucid review of the work of Green, Rivlin and Spencer and extensions of their theory, were presented by Pipkin [5]. He gave the explicit form of the functional when it is expanded into terms of various powers of the time derivative of the finite strain tensor. Pipkin also noted that for the case of small displacements and small rotations the constitutive equation may be written either in a relaxation form (in which the stress tensor is expressed as a functional of the infinitesimal strain tensor) or in a creep form (the infinitesimal strain tensor being expressed as a functional of the stress tensor.)

The relaxation or creep functions characterizing the material behaviour (and which are the kernels appearing in the multiple integral representation of the constitutive equation) must be evaluated from experiments. The extensive testing program required to determine the material functions for a particular material has not yet been undertaken although some studies have been performed which have provided a limited amount of information regarding the form of these functions.

Lifshitz [6] made use of a multiple integral representation for the description of the constitutive equation for polyethylene. Creep tests in tension and torsion were conducted. Each type of test used a single specimen and after a test at a particular stress value the specimen was annealed and another creep test was conducted on the same specimen at a different stress value. The traces of the first, second and third order creep kernel functions were obtained from the tension tests and the traces of two other material functions were obtained from the torsion tests. (The trace of a function of n arguments is obtained by setting all n arguments equal.) Neither strain due to more than one step input stress, nor to combined tension-torsion stress states were obtained. The forms of the second and third order creep kernel functions for non-equal arguments were not obtained. However, important results regarding the type and magnitude of the nonlinearity of polyethylene were obtained.

The results of a similar testing program using a single specimen of polyvinyl chloride copolymer plastic were recently reported by Onaran and

Findley [7]. They conducted combined tension and torsion tests at various stress levels, but again only single step loading was used so that only traces of the kernel functions could be obtained.

Huang and Lee [8] in a theoretical study of nonlinear viscoelasticity suggest that for short time ranges the second and third order kernel functions can be represented by a few terms of the power series expansion in their arguments. This assumed form for short time ranges is supported by the experimental results of Ward and Onat [9] who subjected a polypropylene monofilament to a number of extensional loading steps. Their experimental creep results could be represented with reasonable accuracy by a third order functional. The nonlinearity of polypropylene was found to increase with load intensity and also with time (i.e., time after initially applying the load.) It was also demonstrated that the observed nonlinearity was due to the physical properties of the material and not to geometric nonlinearities introduced by finite deformations alone.

The linearized superposition principle, first advanced by Boltzmann [10], was applied by Leaderman to approximate the constitutive equation of bakelite [11] and was generalized to approximate the constitutive equation of plasticized polyvinyl chloride [12]. Leaderman indicates [13] that certain discontinuities arise when applying this generalized superposition principle to the results of single-step creep tests and to the results of multistage creep and recovery experiments. He suggests that the nonlinear viscoelastic properties of textile fibers can be described only by a multiple integral representation.

A sequence of load histories, each consisting of a series of step inputs was carried out in a testing program reported by Findley and Khosla [15]. Four unfilled thermoplastics were tested and a Modified Superposition Principle (due to Leaderman [14]) was applied to the experimental results. The predicted strains gave average errors of ten percent and the modified superposition principle was applicable when the load remained constant or increased, but could not be used to predict the negative creep rate observed following a decrease in stress. (A similar loading program applied to concrete was carried out by Ross [16]). Although the results of a number of load histories, each consisting of a series of step inputs, is necessary to define the kernel functions in a multiple integral representation of the constitutive equation for a nonlinear viscoelastic material, the above investigators used them simply as a convenient way of applying a time variable loading pattern.

One of the drawbacks of the use of Volterra-Fréchet representation of a functional to describe constitutive relations of materials was very graphically demonstrated by Wang and Onat [17]. The functional constitutive relation of aluminum at 300° F is apparently "continuous" but not "smooth." Even though this functional theoreticaly could be represented to any degree of accuracy by a Fréchet sum, Wang and Onat's results show that an approximation using only a few terms in such a sum does not give results which can reliably predict the material behavior.

Onat uses the suggestive terms "weakly nonlinear" and "strongly nonlinear" to distinguish between materials such as plastics which have a continuous and smooth constitutive relationship and materials such as steel or aluminum (elastic-plastic materials) which have only a continuous constitutive relationship.

In summary, the Volterra-Fréchet multiple integral representation for the functional constitutive equation for the mechanical behavior of materials with memory has been theoretically investigated by many authors and this formulation has a sound theoretical basis. However, very few comprehensive experimental programs have been undertaken to adequately describe the higher order material kernel functions in such a representation.

In this investigation an attempt will be made to determine the kernel functions in a third order multiple integral representation of the one-dimensional creep form of the constitutive relation. The results of input stresses consisting of more than one step will be used to obtain values of the kernel functions which will be used as a basis for a complete determination of these functions. The practicality of this determination will be discussed. The appropriateness of the third order representation for the creep law will be investigated by performing experiments in which a number of known variable load histories are applied to specimens. The measured response will then be compared to the response predicted by the third order multiple integral representation based on the use of the experimentally determined kernel functions previously obtained.

II. THEORY

2.1 Introduction

Since this study was devoted to the problem of determining the one-dimensional material functions for a viscoelastic material undergoing small strains, and to the applicability of the multiple integral representation of the constitutive equation in the solution of one-dimensional stress analysis problems, the theoretical discussion of the assumed strain-stress law could be restricted to the one-dimensional problem. From the assumption that the stress in the X direction is the only input, a Volterra-Fréchet multiple integral expansion could be taken as a representation of the non-linear functional relating the strain in the X direction to the stress input.

However, a more general approach - that of viewing the one-dimensional small strain problem as a particular case of the three-dimensional finite strain problem - not only gives an insight into the tremendously difficult problem of a complete characterization of the material behavior but also demonstrates the relationship between the kernel functions of a one-dimensional constitutive equation and those appearing in the three-dimensional representation. These relationships then allow the results obtained here to be used for the determination of the kernel functions appearing in the three dimensional stress-strain law -- providing other tests are performed.

2.2 Three-Dimensional Viscoelastic Constitutive Equations

Green and Rivlin [3] and Pipkin [5] have shown that the constitutive equation of simple materials (i.e., materials in which the stress components

$\sigma_{ij}(X_p, t)$ at a given particle at time t are dependent only upon the history of the deformation gradients $\partial x_k(\tau)/\partial X_p$ at the same particle) which are isotropic in the undeformed configuration can be written as

$$\boldsymbol{\sigma} = \mathbf{c}\, \mathbb{F}\left[\underset{-\infty}{\overset{t}{\mathbf{E}}}(\tau)\right] \mathbf{c}^{T} \tag{2.1}$$

where $\mathbb{F}$ is a tensor functional. If $\mathbb{F}$ is completely continuous then we can write:

$$\begin{aligned}
\mathbb{F}\left[\underset{-\infty}{\overset{t}{\mathbf{E}}}(\tau)\right] = & \int_{-\infty}^{t} \left\{ M_1(t,\tau_1)\, \mathrm{I\!I}\, \mathrm{tr}\, \dot{\mathbf{E}}(\tau_1) + M_2(t,\tau_1)\, \dot{\mathbf{E}}(\tau_1) \right\} d\tau_1 \\
& + \int_{-\infty}^{t}\int_{-\infty}^{t} \left\{ M_3(t,\tau_1,\tau_2)\, \mathrm{I\!I}\, \mathrm{tr}\left[\dot{\mathbf{E}}(\tau_1)\dot{\mathbf{E}}(\tau_2)\right] + M_4(t,\tau_1,\tau_2)\, \mathrm{I\!I}\, \mathrm{tr}\, \dot{\mathbf{E}}(\tau_1)\, \mathrm{tr}\, \dot{\mathbf{E}}(\tau_2) \right. \\
& \left. + M_5(t,\tau_1,\tau_2)\, \dot{\mathbf{E}}(\tau_1)\, \mathrm{tr}\, \dot{\mathbf{E}}(\tau_2) + M_6(t,\tau_1,\tau_2)\left[\dot{\mathbf{E}}(\tau_1)\dot{\mathbf{E}}(\tau_2) + \dot{\mathbf{E}}(\tau_2)\dot{\mathbf{E}}(\tau_1)\right] \right\} d\tau_1 d\tau_2 \\
& + \int_{-\infty}^{t}\int_{-\infty}^{t}\int_{-\infty}^{t} \left\{ M_7(t,\tau_1,\tau_2,\tau_3)\, \mathrm{I\!I}\, \mathrm{tr}\left[\dot{\mathbf{E}}(\tau_1)\dot{\mathbf{E}}(\tau_2)\dot{\mathbf{E}}(\tau_3)\right] \right. \\
& + M_8(t,\tau_1,\tau_2,\tau_3)\, \mathrm{I\!I}\, \mathrm{tr}\, \dot{\mathbf{E}}(\tau_1)\, \mathrm{tr}\left[\dot{\mathbf{E}}(\tau_2)\dot{\mathbf{E}}(\tau_3)\right] + M_9(t,\tau_1,\tau_2,\tau_3)\, \mathrm{I\!I}\, \mathrm{tr}\, \dot{\mathbf{E}}(\tau_1)\, \mathrm{tr}\, \dot{\mathbf{E}}(\tau_2)\, \mathrm{tr}\, \dot{\mathbf{E}}(\tau_3) \\
& + M_{10}(t,\tau_1,\tau_2,\tau_3)\, \mathrm{tr}\, \dot{\mathbf{E}}(\tau_3)\left[\dot{\mathbf{E}}(\tau_1)\dot{\mathbf{E}}(\tau_2) + \dot{\mathbf{E}}(\tau_2)\dot{\mathbf{E}}(\tau_1)\right] \\
& + M_{11}(t,\tau_1,\tau_2,\tau_3)\, \dot{\mathbf{E}}(\tau_1)\, \mathrm{tr}\, \dot{\mathbf{E}}(\tau_2)\, \mathrm{tr}\, \dot{\mathbf{E}}(\tau_3) + M_{12}(t,\tau_1,\tau_2,\tau_3)\, \dot{\mathbf{E}}(\tau_1)\, \mathrm{tr}\left[\dot{\mathbf{E}}(\tau_2)\dot{\mathbf{E}}(\tau_3)\right] \\
& \left. + M_{13}(t,\tau_1,\tau_2,\tau_3)\left[\dot{\mathbf{E}}(\tau_1)\dot{\mathbf{E}}(\tau_2)\dot{\mathbf{E}}(\tau_3) + \dot{\mathbf{E}}(\tau_3)\dot{\mathbf{E}}(\tau_2)\dot{\mathbf{E}}(\tau_1)\right] \right\} d\tau_1 d\tau_2 d\tau_3 \\
& + \int_{-\infty}^{t}\int_{-\infty}^{t}\int_{-\infty}^{t}\int_{-\infty}^{t} \cdots\cdots
\end{aligned} \tag{2.2}$$

where:

$$\mathbb{I} = \| \delta_{ij} \|$$

$\mathbf{\sigma}(t) = \| \sigma_{ij}(t) \|$ is the stress tensor in the fixed cartesian coordinate system x, and X_i and x_i are the coordinates of a generic particle at time $t = -\infty$ and time $t = \tau$ respectively,

$$\mathbf{c} = \| \partial x_i(\tau) / \partial X_j \|$$

$$g_{ij}(\tau) = \partial x_k(\tau) / \partial X_i \; \partial x_k(\tau) / \partial X_j$$

$$2E_{ij}(\tau) = g_{ij}(\tau) - \delta_{ij}$$

and

$$2\dot{\mathbf{E}}(\tau) = \| \dot{g}_{pq}(\tau) \| = \left\| \frac{\partial \dot{x}_k(\tau)}{\partial X_p} \frac{\partial x_k(\tau)}{\partial X_q} + \frac{\partial x_k(\tau)}{\partial X_p} \frac{\partial \dot{x}(\tau)}{\partial X_q} \right\|$$

By continuous is roughly meant that neighboring input histories (i.e., input histories which defer only slightly for all times τ) produce neighboring output histories.

The terms in the higher order integrals may be easily written down by considering higher order combinations of the following matrix products and invariants:

$$\begin{gathered}
\dot{\mathbf{E}}(\tau_1) \\
\dot{\mathbf{E}}(\tau_1)\dot{\mathbf{E}}(\tau_2) + \dot{\mathbf{E}}(\tau_2)\dot{\mathbf{E}}(\tau_1) \\
\dot{\mathbf{E}}(\tau_1)\dot{\mathbf{E}}(\tau_2)\dot{\mathbf{E}}(\tau_3) + \dot{\mathbf{E}}(\tau_3)\dot{\mathbf{E}}(\tau_2)\dot{\mathbf{E}}(\tau_1) \\
\dot{\mathbf{E}}(\tau_1)\dot{\mathbf{E}}(\tau_2)\dot{\mathbf{E}}(\tau_3)\dot{\mathbf{E}}(\tau_4) + \dot{\mathbf{E}}(\tau_4)\dot{\mathbf{E}}(\tau_3)\dot{\mathbf{E}}(\tau_2)\dot{\mathbf{E}}(\tau_1) \\
\dot{\mathbf{E}}(\tau_1)\dot{\mathbf{E}}(\tau_2)\dot{\mathbf{E}}(\tau_3)\dot{\mathbf{E}}(\tau_4)\dot{\mathbf{E}}(\tau_5) + \dot{\mathbf{E}}(\tau_5)\dot{\mathbf{E}}(\tau_4)\dot{\mathbf{E}}(\tau_3)\dot{\mathbf{E}}(\tau_2)\dot{\mathbf{E}}(\tau_1)
\end{gathered} \tag{2.3}$$

$$
\begin{aligned}
&tr\ \dot{E}(\tau_1)\\
&tr\left[\dot{E}(\tau_1)\dot{E}(\tau_2)\right]\\
&tr\left[\dot{E}(\tau_1)\dot{E}(\tau_2)\dot{E}(\tau_3)\right]\\
&tr\left[\dot{E}(\tau_1)\dot{E}(\tau_2)\dot{E}(\tau_3)\dot{E}(\tau_4)\right]\\
&tr\left[\dot{E}(\tau_1)\dot{E}(\tau_2)\dot{E}(\tau_3)\dot{E}(\tau_4)\dot{E}(\tau_5)\right]\\
&tr\left[\dot{E}(\tau_1)\dot{E}(\tau_2)\dot{E}(\tau_3)\dot{E}(\tau_4)\dot{E}(\tau_5)\dot{E}(\tau_6)\right]
\end{aligned}
\qquad (2.4)
$$

If the material is in a quiescent state prior to time zero, with the application of the input commencing at time zero, then the range of integration may be changed from $(-\infty, t)$ to $(0, t)$.

For non-aging materials, that is, materials for which the form of the response is dependent on the form of the input but not dependent upon the time at which this form was first applied, the material functions M_i are no longer dependent on $(t, \tau_1, \tau_2, \ldots\ldots \tau_n)$ but are only dependent on the time differences $t-\tau_1$ etc. This means, for example, that the kernel function M_4 is reduced from a function of three arguments to a function of the two arguments $t-\tau_1$, $t-\tau_2$. Furthermore, without any loss in generality, M_4 may be assumed symmetric with respect to each argument since its multiplier $\mathrm{II}\, tr\dot{E}(\tau_1)\, tr\dot{E}(\tau_2)$ is symmetric with respect to τ_1 and τ_2 . It should be noted that, in general, all of the kernel functions can not be assumed to have such a complete symmetry with respect to their arguments.

2.3 Further Reduction in the Required Number of Kernel Functions

The Generalized Cayley-Hamilton theorem obtained by Rivlin [4] for arbitrary 3 x 3 matrices A, B, C:

$$
\begin{aligned}
ABC+CBA+BAC+CAB+ACB+BCA = {} & A(\mathrm{tr}BC-\mathrm{tr}B\,\mathrm{tr}C) + B(\mathrm{tr}AC-\mathrm{tr}A\,\mathrm{tr}C) \\
& + C(\mathrm{tr}AB-\mathrm{tr}A\,\mathrm{tr}B) + (BC+CB)\mathrm{tr}A + (AC+CA)\mathrm{tr}B + (AB+BA)\mathrm{tr}C \\
& + \mathrm{II}\left[\mathrm{tr}A\,\mathrm{tr}B\,\mathrm{tr}C-\mathrm{tr}A\,\mathrm{tr}BC-\mathrm{tr}B\,\mathrm{tr}AC-\mathrm{tr}C\,\mathrm{tr}AB+\mathrm{tr}ABC+\mathrm{tr}CBA\right]
\end{aligned}
\tag{2.5}
$$

together with the natural symmetries of the various kernel functions with respect to their arguments provides a means for further reducing the number of kernel functions in the third and higher order terms.

The kernel functions M_7 and M_9 may be taken as symmetric with respect to all three arguments. Equation 2-5 may then be used to express either one of the integrals over M_7 or M_9 in terms of the remaining third order integrals.

It should be noted that for certain particular materials all the kernel functions may be completely symmetric with respect to all arguments. For these cases, Rivlin's theory of matrix invariants may be used to show that the only matrix products and invariants that need be considered in the expansion of $\mathbb{F}$ are:

$$
\begin{gathered}
\dot{E}(\tau_1) \\
\dot{E}(\tau_1)\dot{E}(\tau_2) + \dot{E}(\tau_2)\dot{E}(\tau_1)
\end{gathered}
\tag{2.6}
$$

$$
\begin{gathered}
\mathrm{tr}\,\dot{E}(\tau_1) \\
\mathrm{tr}\left[\dot{E}(\tau_1)\dot{E}(\tau_2)\right] \\
\mathrm{tr}\left[\dot{E}(\tau_1)\dot{E}(\tau_2)\dot{E}(\tau_3)\right]
\end{gathered}
\tag{2.7}
$$

Such a drastic reduction in the number of matrix products and invariants to be considered reduces the number of material kernel functions in the fourth and higher order integrals, but does not reduce the number of kernel functions in the linear, quadratic or cubic integrals.

The number of materials functions required for the characterization of an isotropic viscoelastic solid are:

two linear or single integral functions (functions of one variable)

four quadratic functions (functions of two variables), and

six cubic functions (functions of three variables)

It may be seen that for the third order theory there is a direct correspondence between the number of required kernel functions for a viscoelastic solid and the number of required materials constants for a Cauchy elastic solid (see Ref. [18]).

This direct correspondence between the number of material functions for a viscoelastic solid and the number of constants for a Cauchy elastic solid would continue for all higher order terms if the viscoelastic material were of the special type that could be characterized using only the terms of the form shown in Equation 2-6 and Equation 2-7. In the general case, however, this would not be true.

2.4 Creep Integral Representation

The creep integral representation of the constitutive equation for a nonlinear viscoelastic solid can be obtained from the preceding stress relaxation formulation by rewriting Equation 2.1 as

$$\mathbf{C}^{-1}\boldsymbol{\sigma}\,\mathbf{C}^{-1^{T}} = \mathbf{F}\left[\int_{-\infty}^{t}\mathbf{E}(\tau)\right] \tag{2.8}$$

If we now assume that Equation 2.8 has an inverse, then it must be of the form

$$\mathbb{E}(t) = \mathbb{H}\left[\int_{-\infty}^{t} \Phi^{-1} \dot{\Phi} \Phi^{-1T}\right] \tag{2.9}$$

and following exactly the same arguments used in developing a representation for $\mathbb{F}$ in Equation 2.1 it can be shown that $\mathbb{H}$ may be represented by a sum of multiple integrals given by replacing $\dot{\mathbb{E}}(\tau)$ in Equation 2.2 by $\frac{\partial}{\partial \tau}\left[\Phi^{-1} \dot{\Phi} \Phi^{-1T}\right]$.

That is:

$$\begin{aligned}
\mathbb{E}(t) = & \int_{-\infty}^{t} \left\{ J_1(t;\tau_1)\, \mathbb{II}\, tr\, \dot{\Pi}(\tau_1) + J_2(t;\tau_1)\, \dot{\Pi}(\tau_1) \right\} d\tau_1 \\
& + \int_{-\infty-\infty}^{tt} \left\{ J_3(t;\tau_1,\tau_2)\, \mathbb{II}\, tr\left[\dot{\Pi}(\tau_1)\dot{\Pi}(\tau_2)\right] + J_4(t;\tau_1,\tau_2)\, \mathbb{II}\, tr\,\dot{\Pi}(\tau_1)\, tr\,\dot{\Pi}(\tau_2) \right. \\
& + J_5(t;\tau_1,\tau_2)\, \dot{\Pi}(\tau_1)\, tr\,\dot{\Pi}(\tau_2) + J_6(t;\tau_1,\tau_2)\left[\dot{\Pi}(\tau_1)\dot{\Pi}(\tau_2) + \dot{\Pi}(\tau_2)\dot{\Pi}(\tau_1)\right] \left. \right\} d\tau_1 d\tau_2 \\
& + \int_{-\infty-\infty-\infty}^{ttt} \left\{ J_7(t;\tau_1,\tau_2,\tau_3)\, \mathbb{II}\, tr\left[\dot{\Pi}(\tau_1)\dot{\Pi}(\tau_2)\dot{\Pi}(\tau_3)\right] \right. \\
& + J_8(t;\tau_1,\tau_2,\tau_3)\, \mathbb{II}\, tr\,\dot{\Pi}(\tau_1)\, tr\left[\dot{\Pi}(\tau_2)\dot{\Pi}(\tau_3)\right] + J_{10}(t;\tau_1,\tau_2,\tau_3)\, tr\,\dot{\Pi}(\tau_3)\left[\dot{\Pi}(\tau_1)\dot{\Pi}(\tau_2) + \dot{\Pi}(\tau_2)\dot{\Pi}(\tau_1)\right] \\
& + J_{11}(t;\tau_1,\tau_2,\tau_3)\, \dot{\Pi}(\tau_1)\, tr\,\dot{\Pi}(\tau_2)\, tr\,\dot{\Pi}(\tau_3) + J_{12}(t;\tau_1,\tau_2,\tau_3)\, \dot{\Pi}(\tau_1)\, tr\left[\dot{\Pi}(\tau_2)\dot{\Pi}(\tau_3)\right] \\
& \left. + J_{13}(t;\tau_1,\tau_2,\tau_3)\left[\dot{\Pi}(\tau_1)\dot{\Pi}(\tau_2)\dot{\Pi}(\tau_3) + \dot{\Pi}(\tau_3)\dot{\Pi}(\tau_2)\dot{\Pi}(\tau_1)\right] \right\} d\tau_1 d\tau_2 d\tau_3 + \int_{-\infty-\infty-\infty-\infty}^{tttt} \cdots
\end{aligned} \tag{2.10}$$

where

$$\Pi = \Phi^{-1} \dot{\Phi} \Phi^{-1T} \tag{2.11}$$

The legitimacy of this representation depends (in part) upon the assumption of continuity of the functional $\mathcal{H}$. Whereas in the stress relaxation formulation it was necessary that neighboring strain histories produce neighboring stress histories, the creep integral formulation requires that neighboring stress histories produce neighboring strain histories. An ideal elastic-plastic material is a simple example of a material for which this continuity condition would not apply. The difficulty experienced by Wang and Onat [17] in attempting to apply the Volterra-Fréchet representation to aluminum at 300° F is probably due to such a nearly abrupt change in behavior of the material in the vicinity of the idealized yield stress of the aluminum.

This possible restriction of the creep integral representation is perhaps of less importance than the fact that measures of the deformation appear on both sides of constitutive equation 2.10. The desired output (the finite strain tensor $\mathbf{E}$) is not only dependent upon the stress input, but also on the deformation gradient matrix $\mathbf{C}$. For small deformations the deformation gradient matrix essentially reduces to the identity matrix, but no such reduction is possible for finite deformations.

2.5 One-Dimensional Viscoelastic Constitutive Equations

As pointed out in the previous section, twelve material functions appear in the three-dimensional third order Volterra-Fréchet expansion of the constitutive equation for a viscoelastic material. The laborious task of determining such a large number of material functions for a particular

material must be accomplished in simple stages. Firstly, one-dimensional creep or relaxation tests may be performed. Secondly, two-dimensional test results are required and finally, an examination of the response of the material to three-dimensional inputs would be required.

In a one-dimensional creep test the stress history is of the form

$$\sigma_{11}(t) = \sigma(t)$$
$$\sigma_{ij}(t) = 0 \quad \text{all other } i,j \tag{2.12}$$

If the material is isotropic, then this stress state must produce a deformation of the form

$$\begin{aligned} x_1(t) &= x_1(X_1, t) \\ x_2(t) &= x_2(X_2, t) \\ x_3(t) &= x_3(X_3, t) \end{aligned} \tag{2.13}$$

This follows from the fact that rotations of the coordinate system about the x_1 axis or translations in the $x_2 x_3$ plane give no changes in the stress state or the material properties. Hence $\mathbf{c}$ is diagonal and

$$\mathbf{T}(t) = \mathbf{c}^{-1}\boldsymbol{\sigma}\mathbf{c}^{-1T} = \begin{Vmatrix} \frac{\partial X_1}{\partial x_1}(t)\,\frac{\partial X_1}{\partial x_1}(t)\,\sigma_{11}(t) & 0 & 0 \\ 0 & 0 & 0 \\ 0 & 0 & 0 \end{Vmatrix} \tag{2.14}$$

so that Equation 2-10 reduces to

$$E_{11}(t) = \int_{-\infty}^{t} \left\{ J_1(t,\tau_1) + J_2(t,\tau_1) \right\} \dot{T}_{11}(\tau_1)\, d\tau_1$$
$$+ \int_{-\infty-\infty}^{t\,t} \left\{ J_3(t,\tau_1,\tau_2) + J_4(t,\tau_1,\tau_2) + J_5(t,\tau_1,\tau_2) + 2J_6(t,\tau_1,\tau_2) \right\} \dot{T}_{11}(\tau_1)\dot{T}_{11}(\tau_2)\, d\tau_1 d\tau_2$$
$$+ \int_{-\infty-\infty-\infty}^{t\,t\,t} \left\{ J_7(t,\tau_1,\tau_2,\tau_3) + J_8(t,\tau_1,\tau_2,\tau_3) + 2J_{10}(t,\tau_1,\tau_2,\tau_3) + J_{11}(t,\tau_1,\tau_2,\tau_3) + J_{12}(t,\tau_1,\tau_2,\tau_3) \right.$$
$$\left. + 2\, J_{13}(t,\tau_1,\tau_2,\tau_3) \right\} \dot{T}_{11}(\tau_1)\dot{T}_{11}(\tau_2)\dot{T}_{11}(\tau_3)\, d\tau_1 d\tau_2 d\tau_3 \qquad (2.15a)$$
$$+ \int_{-\infty-\infty-\infty-\infty}^{t\,t\,t\,t} \cdots$$

$$E_{22}(t) = E_{33}(t) = \int_{-\infty}^{t} \left\{ J_1(t,\tau_1) \right\} \dot{T}_{11}(\tau_1)\, d\tau_1$$
$$+ \int_{-\infty-\infty}^{t\,t} \left\{ J_3(t,\tau_1,\tau_2) + J_4(t,\tau_1,\tau_2) \right\} \dot{T}_{11}(\tau_1)\dot{T}_{11}(\tau_2)\, d\tau_1 d\tau_2 \qquad (2.15b)$$
$$+ \int_{-\infty-\infty-\infty}^{t\,t\,t} \left\{ J_7(t,\tau_1,\tau_2,\tau_3) + J_8(t,\tau_1,\tau_2,\tau_3) \right\} \dot{T}_{11}(\tau_1)\dot{T}_{11}(\tau_2)\dot{T}_{11}(\tau_3)\, d\tau_1 d\tau_2 d\tau_3$$
$$+ \cdots$$

$$E_{ij}(t) = 0 \qquad i \neq j \qquad (2.15c)$$

The expression 2-15a is one dimensional in the sense that the strain in the x_1 direction is dependent only on the past history of the stress in the x_1 direction. The measured response $E_{11}(t)$ due to various input stresses $\sigma_{11}(t)$ will provide information for the determination of the

combinations of third order kernel functions J_i contained in the braces.

For a one-dimensional relaxation test with the deformation history specified by

$$\begin{aligned} x_1(t) &= X_1 + f(X_1, t) \\ x_2(t) &= X_2 \\ x_3(t) &= X_3 \end{aligned} \tag{2.16}$$

Equation 2.2 gives a representation for $T_{11}(t)$ very similar to the above results for $E_{11}(t)$.

$$\begin{aligned} T_{11}(t) = & \int_{-\infty}^{t} \left\{ M_1(t,\tau_1) + M_2(t,\tau_1) \right\} \dot{E}_{11}(\tau_1)\, d\tau_1 \\ & + \int_{-\infty}^{t}\int_{-\infty}^{t} \left\{ M_3(t,\tau_1,\tau_2) + M_4(t,\tau_1,\tau_2) + M_5(t,\tau_1,\tau_2) + 2M_6(t,\tau_1,\tau_2) \right\} \dot{E}_{11}(\tau_1)\dot{E}_{11}(\tau_2)\, d\tau_1 d\tau_2 \\ & + \int_{-\infty}^{t}\int_{-\infty}^{t}\int_{-\infty}^{t} \left\{ M_8(t,\tau_1,\tau_2,\tau_3) + 2M_{10}(t,\tau_1,\tau_2,\tau_3) + M_{11}(t,\tau_1,\tau_3,\tau_3) + M_7(t,\tau_1,\tau_2,\tau_3) \right. \\ & \qquad \left. + M_{12}(t,\tau_1,\tau_2,\tau_3) + 2M_{13}(t,\tau_1,\tau_2,\tau_3) \right\} \dot{E}_{11}(\tau_1)\dot{E}_{11}(\tau_2)\dot{E}_{11}(\tau_3)\, d\tau_1 d\tau_2 d\tau_3 \\ & + \int_{-\infty}^{t}\int_{-\infty}^{t}\int_{-\infty}^{t}\int_{-\infty}^{t} \cdots\cdots \end{aligned} \tag{2.17}$$

However, the more common types of one dimensional relaxation tests are those in which the $x_1(t)$ deformation history is prescribed and the two stresses $\sigma_{22}(t)$ and $\sigma_{33}(t)$ are maintained at zero values. For this case we assume that the deformation

$$x_1(t) = X_1[1 + f(t)]$$
$$x_2(t) = X_2[1 + g(t)]$$
$$x_3(t) = X_3[1 + g(t)] \qquad (2.18)$$

is associated with the stress output

$$\sigma_{11}(t) = \sigma(t)$$
$$\sigma_{ij}(t) = 0 \quad \text{all other } i,j \qquad (2.19)$$

where we view f as arbitrary and g prescribed by the condition that

$$\sigma_{22}(t) = \sigma_{33}(t) = 0$$

Then

$$\mathfrak{C} = \begin{Vmatrix} 1+f & 0 & 0 \\ 0 & 1+g & 0 \\ 0 & 0 & 1+g \end{Vmatrix} \qquad (2.20)$$

and

$$\dot{E}(t) = \begin{Vmatrix} \dot{f}(1+f) & 0 & 0 \\ 0 & \dot{g}(1+g) & 0 \\ 0 & 0 & \dot{g}(1+g) \end{Vmatrix} \qquad (2.21)$$

so that we obtain

$$\frac{\sigma_{11}(t)}{(1+f)^2} = \int_{-\infty}^{t} \left\{ M_1\left[\dot{E}_{11}(\tau_1)+2\dot{E}_{22}(\tau_1)\right] + M_2\dot{E}_{11}(\tau_1) \right\} d\tau_1$$

$$+\int_{-\infty}^{t}\int_{-\infty}^{t} \left\{ M_3\left[\dot{E}_{11}(\tau_1)\dot{E}_{11}(\tau_2)+2\dot{E}_{22}(\tau_1)\dot{E}_{22}(\tau_2)\right] + M_4\left[\dot{E}_{11}(\tau_1)+2\dot{E}_{22}(\tau_1)\right]\left[\dot{E}_{11}(\tau_2)+2\dot{E}_{22}(\tau_2)\right] \right.$$

$$\left. + M_5\left[\dot{E}_{11}(\tau_2)+2\dot{E}_{22}(\tau_2)\right]\dot{E}_{11}(\tau_1) + 2M_6\dot{E}_{11}(\tau_1)\dot{E}_{11}(\tau_2) \right\} d\tau_1 d\tau_2$$

$$+\int_{-\infty}^{t}\int_{-\infty}^{t}\int_{-\infty}^{t} \left\{ M_7\left[\dot{E}_{11}(\tau_1)\dot{E}_{11}(\tau_2)\dot{E}_{11}(\tau_3)+2\dot{E}_{22}(\tau_1)\dot{E}_{22}(\tau_2)\dot{E}_{22}(\tau_3)\right] + M_8\left[\dot{E}_{11}(\tau_1)+2\dot{E}_{22}(\tau_1)\right]\left[\dot{E}_{11}(\tau_2)\dot{E}_{11}(\tau_3)+2\dot{E}_{22}(\tau_2)\dot{E}_{22}(\tau_3)\right] \right.$$

$$+2M_{10}\left[\dot{E}_{11}(\tau_3)+2\dot{E}_{22}(\tau_3)\right]\dot{E}_{11}(\tau_1)\dot{E}_{11}(\tau_2) + M_{12}\left[\dot{E}_{11}(\tau_2)\dot{E}_{11}(\tau_3)+2\dot{E}_{22}(\tau_2)\dot{E}_{22}(\tau_3)\right]\dot{E}_{11}(\tau_1)$$

$$\left. + M_{11}\left[\dot{E}_{11}(\tau_2)+2\dot{E}_{22}(\tau_1)\right]\left[\dot{E}_{11}(\tau_3)+2\dot{E}_{22}(\tau_3)\right]\dot{E}_{11}(\tau_1) + 2M_{13}\dot{E}_{11}(\tau_1)\dot{E}_{11}(\tau_2)\dot{E}_{11}(\tau_3) \right\} d\tau_1 d\tau_2 d\tau_3$$

$$+ \cdots \qquad (2.22a)$$

and

$$\frac{\sigma_{22}(t)}{(1+g)^2} = 0 = \int_{-\infty}^{t} \left\{ M_1\left[\dot{E}_{11}(\tau_1)+2\dot{E}_{22}(\tau_1)\right] + M_2\dot{E}_{22}(\tau_1) \right\} d\tau_1$$

$$+\int_{-\infty}^{t}\int_{-\infty}^{t} \left\{ M_3\left[\dot{E}_{11}(\tau_1)\dot{E}_{11}(\tau_2)+2\dot{E}_{22}(\tau_1)\dot{E}_{22}(\tau_2)\right] + M_4\left[\dot{E}_{11}(\tau_1)+2\dot{E}_{22}(\tau_1)\right]\left[\dot{E}_{11}(\tau_2)+2\dot{E}_{22}(\tau_2)\right] \right.$$

$$\left. + M_5\left[\dot{E}_{11}(\tau_2)+2\dot{E}_{22}(\tau_2)\right]\dot{E}_{22}(\tau_2) + 2M_6\dot{E}_{22}(\tau_1)\dot{E}_{22}(\tau_2) \right\} d\tau_1 d\tau_2$$

$$+\int_{-\infty}^{t}\int_{-\infty}^{t}\int_{-\infty}^{t} \cdots\cdots + \qquad (2.22b)$$

where the arguments of the functions M_i have not been written.

In this case it is necessary to have measured values of the two "inputs" f and g (from which E can be calculated) as well as the output $\sigma_{11}(t)$ in order to obtain information regarding the form of the three dimensional relaxation kernel functions M_i . Theoretically, it would appear that Equation 2.22b could be used to eliminate g (and therefore E_{22}) from Equation 2.22a in order to express $\sigma_{11}(t)$ as a functional of $E_{11}(t)$:

$$\frac{\sigma_{11}(t)}{(1+f)^2} = \int_{-\infty}^{t} M_1^*(t,\tau_1)\dot{E}_{11}(\tau_1)\,d\tau_1 + \int_{-\infty}^{t}\int_{-\infty}^{t} M_2^*(t,\tau_1,\tau_2)\dot{E}_{11}(\tau_1)\dot{E}_{11}(\tau_2)\,d\tau_1 d\tau_2 + \cdots \qquad (2.23)$$

From this point of view, a relaxation test could also be considered as a one-dimensional test. However, there is no simple relation between the kernel functions M_i^* in this formulation and the kernel functions M_i in the general three-dimensional relaxation formulation.

2.6 Discussion of the Problem of Determination of the One-Dimensional Creep Functions

For the case of infinitesimal deformations, the one-dimensional creep-integral constitutive equation 2.15a may be written as

$$e(t) = \int_0^t K_1(t-\tau)\dot{\sigma}(\tau)\,d\tau + \int_0^t\int_0^t K_2(t-\tau_1,t-\tau_2)\dot{\sigma}(\tau_1)\dot{\sigma}(\tau_2)\,d\tau_1 d\tau_2 + \int_0^t\int_0^t\int_0^t K_3(t-\tau_1,t-\tau_2,t-\tau_3)\dot{\sigma}(\tau_1)\dot{\sigma}(\tau_2)\dot{\sigma}(\tau_3)\,d\tau_1 d\tau_2 d\tau_3 + \cdots \qquad (2.24)$$

where the strain $e(t)$ is the change in length of the specimen at time t divided by the original length, and the stress $\sigma(t)$ is the tensile force at time t divided by the original area. The kernel functions K_i will be

called the one-dimensional creep functions and are related to the three dimensional creep functions J_i in the following way:

$$
\begin{aligned}
K_1(t) &= J_1(t) + J_2(t) \\
K_2(t_1,t_2) &= J_3(t_1,t_2) + J_4(t_1,t_2) + J_5(t_1,t_2) + 2J_6(t_1,t_2) \\
K_3(t_1,t_2,t_3) &= J_7(t_1,t_2,t_3) + J_8(t_1,t_2,t_3) + 2J_{10}(t_1,t_2,t_3) \\
&\quad + J_{11}(t_1,t_2,t_3) + J_{12}(t_1,t_2,t_3) + 2J_{13}(t_1,t_2,t_3)
\end{aligned}
\tag{2.25}
$$

The lower limit of integration in Equation 2.24 is taken as zero since the material is assumed stress free and undisturbed prior to the time zero. The arguments of the kernel functions are $t-\tau_1$, $t-\tau_2$, etc., since the material is assumed to be non-aging. All of the kernel functions may be assumed to be symmetric with respect to all arguments. The upper limits of integration are the present time t since the future values of the input cannot influence the present value of the output. By observing the form of each integral we note that the value of a kernel function when any of its arguments are negative never enters into the evaluation of the integral. From these considerations we can see that the kernel functions are completely determined when we have their values for the following situations:

$$
\begin{aligned}
&K_1(t) \qquad t \geq 0 \\
&K_2(t_1,t_2) \qquad t_1 \geq t_2 \geq 0 \\
&K_3(t_1,t_2,t_3) \qquad t_1 \geq t_2 \geq t_3 \geq 0
\end{aligned}
\tag{2.26}
$$

The type of input stresses $\sigma(t)$ that may be used to determine the kernel functions is arbitrary. However, the form of the representation 2.24 is particularly suited to step inputs, since for such loads we do not have to deal with integral equations. For example, if

$$\sigma(t) = \sigma_1 H(t) \tag{2.27}$$

where $H(t)$ denotes the Heaviside step function

$$H(t) = \begin{cases} 0 & t < 0 \\ 1 & t \geq 0 \end{cases} \tag{2.28}$$

then Equation 2.24 directly reduces to

$$e(t) = \sigma_1 K_1(t) + \sigma_1^2 K_2(t,t) + \sigma_1^3 K_3(t,t,t) + \cdots \tag{2.29}$$

Thus, the traces of the kernel functions may be determined relatively easily from this convenient expression.

A number of authors have discussed methods for the experimental determinatio of the kernel functions (see Ward and Onat [9], Onaran and Findley [7]). Lockett [19] investigated the type and number of experiments required to determine the kernel functions in a third order representation. Investigators in the field of electrical control systems have also studied the problem of representation and use of functionals in representing non-linear systems. Brilliant [20], George [21], and Schetzen [22] describe the method of finite differences as applied to a functional relationship.

In most of these investigations the representation corresponding to Equation 2.24 has been terminated after a finite number of terms and then the tacit assumption is made that this finite order expansion represents the system exactly. In this investigation, only a finite number of terms in the representation 2.24 will be considered. However, it will always be kept in mind that this finite order expansion only approximates the system under investigation.

The infinite order integral representation as compared to the finite order representation can be viewed as analogous to a Taylor series expansion of a function (in which case the constants are determined independently of one another) as compared to a Stone-Weierstrass polynomial approximation of a function (in which case the constants are dependent on the order of the polynomial and on the range of approximation). The finite order approximation is used in this investigation and the kernel functions are found by attempting to fit this finite order integral expansion to a wide range of inputs.

If $e^{+}(t)$ is the strain output due to a stress input of $+\sigma(t)$ and $e^{-}(t)$ is the strain output due to a stress input of $-\sigma(t)$ then from Equation 2.24 we obtain

$$\xi(t) = \frac{e^{+}(t) + e^{-}(t)}{2} = \int_0^t \int_0^t K_2(t-\tau_1, t-\tau_2)\dot{\sigma}(\tau_1)\dot{\sigma}(\tau_2)\, d\tau_1\, d\tau_2 + \int_0^t \int_0^t \int_0^t \int_0^t \cdots + \qquad (2.30a)$$

and

$$\epsilon(t) = \frac{e^{+}(t) - e^{-}(t)}{2} = \int_0^t K_1(t-\tau)\,\dot{\sigma}(\tau)\,d\tau + \int_0^t\int_0^t\int_0^t K_3(t-\tau_1, t-\tau_2, t-\tau_3)\,\dot{\sigma}(\tau_1)\dot{\sigma}(\tau_2)\dot{\sigma}(\tau_3)\,d\tau_1 d\tau_2 d\tau_3 + \cdots \tag{2.30b}$$

For most materials $e^{+}(t)$ will be approximately equal to $-e^{-}(t)$ so that $\xi(t)$ will be much smaller than $\epsilon(t)$. We will terminate Equation 2.30a after one term and Equation 2.30b after two terms (i.e., we use a three term truncation of Equation 2.24) and investigate the method of determining the creep kernel functions in this finite order approximation.

In the following sections a "measured" output $\xi(t)$ or $\epsilon(t)$ does not refer to the actual output of a real test, but rather to the above appropriate combinations of the measured strain responses of the viscoelastic material tested.

2.7 Determination of the Even Order Creep Function

The truncation of Equation 2.30a gives the creep integral equation involving $K_2(t_1, t_2)$.

$$\xi(t) = \int_0^t\int_0^t K_2(t-\tau_1, t-\tau_2)\,\dot{\sigma}(\tau_1)\,\dot{\sigma}(\tau_2)\,d\tau_1\,d\tau_2 \tag{2.31}$$

For a standard creep test under constant stress σ_i, the input is given by:

$$\sigma(t) = \sigma_i\,H(t) \tag{2.32}$$

For this input Equation 2.31 reduces to:

$$\xi(t) = \sigma_i^2 K_2(t,t) \tag{2.33}$$

The corresponding measured output of the material tested will be denoted by $\xi_i(t)$. Since the constitutive equation of the material is unlikely to be of exactly third order, this output actually will be given by:

$$\xi_i(t) = \sigma_i^2 K_2(t,t) + \sigma_i^4 K_4(t,t,t,t) + \sigma_i^6 K_6(t,t,t,t,t,t) + \cdots \tag{2.34}$$

The second order kernel function in the truncated integral formulation may be determined by setting the "error",

$$\xi_i(t) - \sigma_i^2 K_2(t,t) \tag{2.35}$$

equal to zero for a particular value of σ_i or by minimizing this error with respect to some norm over a range of input values σ_i. Naturally the value of $K_2(t,t)$ will depend not only upon the minimizing condition but also upon the range of σ_i over which this minimization takes place. In this investigation we will use a least-squares procedure for the determination of the kernel functions. That is, for every fixed value of t, we will require that $K_2(t,t)$ minimize the following expression:

$$E = \sum_i \left[\xi_i(t) - \sigma_i^2 K_2(t,t) \right]^2 \tag{2.36}$$

where the summation is taken over the range of input stresses σ_i utilized.

For E to be a minimum we must have

$$-\frac{1}{2}\frac{\partial E}{\partial K_2(t,t)} = \sum_i \sigma_i^2 \left[\xi_i(t) - \sigma_i^2 K_2(t,t)\right] = 0 \tag{2.37}$$

It can be seen that by determining $K_2(t,t)$ to satisfy this equation for each fixed value of t we have traced out the value of $K_2(t_1,t_2)$ when both its arguments are equal (see Fig. 1).

To obtain values of this kernel function at other points within the t_1, t_2 plane we must carry out a generalized creep test consisting of two step input stresses. That is, we must apply a stress history of the form

$$\sigma(t) = \sigma_i H(t) + \sigma_j H(t-T) \tag{2.38}$$

where σ_i and σ_j are constants. For this input Equation (2.31) yields (for $t \geq T$)

$$\xi(t) = \sigma_i^2 K_2(t,t) + 2\sigma_i\sigma_j K_2(t,t-T) + \sigma_j^2 K_2(t-T,t-T) \tag{2.39}$$

where the symmetry of $K_2(t_1,t_2)$ with respect to its arguments has been used. Note that if $K_2(t,t)$ is known then so is $K_2(t-T,t-T)$. Denoting the measured output strain of the material due to this two step input stress loading as $\xi_{ij}(t)$ we can again form the sum of the squares of the errors:

$$E = \sum_i \sum_j \left[\xi_{ij}(t) - \sigma_i^2 K_2(t,t) - 2\sigma_i\sigma_j K_2(t,t-T) - \sigma_j^2 K_2(t-T,t-T)\right]^2 \tag{2.40}$$

The only unknown in this expression is $K_2(t,t-T)$ so that for each fixed value of t, $K_2(t,t-T)$ must satisfy:

$$-\frac{1}{4}\frac{\partial E}{\partial K_2(t,t-T)} = \sum_i \sum_j \sigma_i\sigma_j \left[\xi_{ij}(t) - \sigma_i^2 K_2(t,t) - 2\sigma_i\sigma_j K_2(t,t-T) - \sigma_j^2 K_2(t-T,t-T)\right] = 0 \tag{2.41a}$$

which may also be written as

$$\sum_i \sum_j \sigma_i \sigma_j \left[\xi_{ij}(t) - \overline{\xi}_i(t) - \overline{\xi}_j(t-T) - 2\sigma_i \sigma_j K_2(t, t-T) \right] = 0 \qquad (2.41b)$$

where $\xi_{ij}(t)$ is the measured output due to $\sigma_i H(t) + \sigma_j H(t-T)$ and $\overline{\xi}_i(t)$ is the output of Equation 2.31 due to $\sigma_i H(t)$.

The summations in Equations 2.41a and 2.41b are over the sets of inputs $\{\sigma_i \sigma_j\}$ utilized in the experiments.

$K_2 (t, t-T)$ is the value of the function $K_2 (t_1, t_2)$ along a line in the (t_1, t_2) plane which is parallel to the (t, t) line and which intersects the t_1 axis at $t_1 = T$ (see Fig. 1). A complete determination of $K_2 (t_1, t_2)$ would necessitate tracing out the function $K_2(t, t-T)$ for all positive values of the variable T. Fortunately, the second order creep function for many materials is sufficiently smooth so that only a few values of T need be investigated. The non-determined values of the function may then be obtained by interpolation or extrapolation from the determined values.

2.8 Determination of the Odd Order Creep Functions

The two kernel functions in the truncated form of Equation 2.30b:

$$\epsilon(t) = \int_0^t K_1(t-\tau)\, \dot{\sigma}(\tau)\, d\tau + \int_0^t \int_0^t \int_0^t K_3(t-\tau_1, t-\tau_2, t-\tau_3)\, \dot{\sigma}(\tau_1)\, \dot{\sigma}(\tau_2)\, \dot{\sigma}(\tau_3)\, d\tau_1\, d\tau_2\, d\tau_3 \qquad (2.42)$$

are determined in a manner analogous to the procedure described above. A least-squares minimization criterion is again used to determine the two kernel functions to fit the test results of generalized creep tests.

Since $K_3(t_1,t_2,t_3)$ is a function of three variables, the response of the system to inputs consisting of three steps must be determined experimentally.

As in the case of the evaluation of $K_2(t_1,t_2)$, single step inputs give outputs from which $K_3(t,t,t)$ may be determined. Two step inputs following each other by a time delay T give results from which $K_3(t,t,t-T)$ and $K_3(t,t-T,t-T)$ may be determined. That is, K_3 is determined along lines which are parallel to the line (t,t,t) in the (t_1,t_2,t_3) space and which intersect the (t_1,t_2) plane at the points $(T,0)$ and (T,T) respectively. Three step inputs following each other by time delays T_1 and T_2, respectively, allow the determination of K_3 along other lines parallel to the (t,t,t) line and which intersect the (t_1,t_2) plane at the point (T_1,T_2). (see Fig. 2). From the relation 2.26 it may be seen that the value of $K_3(t_1,t_2,t_3)$ is required only in the wedge-shaped region of three space shown in Fig. 2, which has the lines (t,t,t), $(t,t,0)$ and $(t,0,0)$ as edges. If a sufficient number of generalized creep tests are performed, $K_3(t_1,t_2,t_3)$ may be determined by interpolation from the traced out values.

For a standard creep test ($\sigma(t) = \sigma_i H(t)$), Equation 2.42 reduces to

$$\epsilon(t) = \sigma_i K_1(t) + \sigma_i^3 K_3(t,t,t) \tag{2.43}$$

Following the same procedure as before we wish to minimize the difference between this expression and the measured output of the system $\epsilon_i(t)$ over the set of test inputs utilized. From

$$E = \sum_i \left[\epsilon_i(t) - \sigma_i K_1(t) - \sigma_i^3 K_3(t,t,t) \right]^2 \tag{2.44}$$

we get two equations for the determination of $K_1(t)$ and $K_3(t,t,t)$

$$-\frac{1}{2}\frac{\partial E}{\partial K_1} = \sum_i \sigma_i \left[\epsilon_i(t) - \sigma_i K_1(t) - \sigma_i^3 K_3(t,t,t)\right] = 0 \tag{2.45a}$$

$$-\frac{1}{2}\frac{\partial E}{\partial K_3} = \sum_i \sigma_i^3 \left[\epsilon_i(t) - \sigma_i K_1(t) - \sigma_i^3 K_3(t,t,t)\right] = 0 \tag{2.45b}$$

For a generalized creep test with input defined by Equation 2.38, Equation 2.42 gives (for $t \geq T$)

$$\epsilon(t) = \sigma_i K_1(t) + \sigma_j K_1(t-T) + \sigma_i^3 K_3(t,t,t) + \sigma_j^3 K_3(t-T,t-T,t-T) + 3\sigma_i^2\sigma_j K_3(t,t,t-T) + 3\sigma_i\sigma_j^2 K_3(t,t-T,t-T) \tag{2.46}$$

Using the notation

$\epsilon_{ij}(t)$ = measured response of the system due to $\sigma_i H(t) + \sigma_j H(t-T)$

$\overline{\epsilon_i}(t)$ = output of Equation 2.42 due to $\sigma_i H(t)$

$= \sigma_i K_1(t) + \sigma_i^3 K_3(t,t,t)$

$\overline{\epsilon_j}(t-T)$ = output of Equation 2.42 due to $\sigma_j H(t-T)$

$= \sigma_j K_1(t-T) + \sigma_j^3 K_3(t-T,t-T,t-T)$

it can be seen that the difference between the measured response and the response given by Equation 2.46 will contain the two unknowns $K_3(t,t,t-T)$ and $K_3(t,t-T,t-T)$. A least squares minimization criteria applied to this "error" yields:

$$\sum_i \sum_j \sigma_i^2\sigma_j \left[\epsilon_{ij}(t) - \overline{\epsilon_i}(t) - \overline{\epsilon_j}(t-T) - 3\sigma_i^2\sigma_j K_3(t,t,t-T) - 3\sigma_i\sigma_j^2 K_3(t,t-T,t-T)\right] = 0 \tag{2.47a}$$

and

$$\sum_i \sum_j \sigma_i \sigma_j^2 \left[\epsilon_{ij}(t) - \bar{\epsilon}_i(t) - \bar{\epsilon}_j(t-\tau) - 3\sigma_i^2 \sigma_j K_3(t,t,t-\tau) - 3\sigma_i \sigma_j^2 K_3(t,t-\tau,t-\tau) \right] = 0 \tag{2.47b}$$

So that $K_3(t,t,t-\tau)$ and $K_3(t,t-\tau,t-\tau)$ may be determined from these equations where the summation is taken over the set of inputs utilized in the experiments.

Equations 2.46 and 2.47 may be used to evaluate $K_3(t_1,t_2,t_3)$ when two or more arguments are the same. The value of this third order kernel function with all three arguments different will occur explicitly in the representation for the strain output due to a three step stress input:

$$\sigma(t) = \sigma_i H(t) + \sigma_j H(t-\tau) + \sigma_k H(t-s) \tag{2.48}$$

For this input Equation 2.42 reduces (for $t \geq s > \tau$) to

$$\begin{aligned} \epsilon(t) = {} & \sigma_i K_1(t) + \sigma_j K_1(t-\tau) + \sigma_k K_1(t-s) \\ & + \sigma_i^3 K_3(t,t,t) + \sigma_j^3 K_3(t-\tau,t-\tau,t-\tau) + \sigma_k^3 K_3(t-s,t-s,t-s) \\ & + 3\sigma_i^2\sigma_j K_3(t,t,t-\tau) + 3\sigma_i^2\sigma_k K_3(t,t,t-s) + 3\sigma_j^2\sigma_k K_3(t-\tau,t-\tau,t-s) \\ & + 3\sigma_j^2\sigma_i K_3(t,t-\tau,t-\tau) + 3\sigma_k^2\sigma_j K_3(t-\tau,t-s,t-s) + 3\sigma_k^2\sigma_i K_3(t,t-s,t-s) \\ & + 6\sigma_i\sigma_j\sigma_k K_3(t,t-\tau,t-s) \end{aligned} \tag{2.49}$$

This expression may be written in a simpler form by noting that this response to a three step input is built up of combinations of responses to single and double step inputs. Let

$\bar{\epsilon}_{ijo}(t)$ denote the output of Equation 2.42 due to

$$\sigma(t) = \sigma_i H(t) + \sigma_j H(t-\tau) \tag{2.50a}$$

$\bar{\epsilon}_{iok}(t)$ denote the output of Equation 2.42 due to

$$\sigma(t) = \sigma_i H(t) + \sigma_k H(t-s) \tag{2.50b}$$

$\bar{\epsilon}_{ojk}(t)$ denote the output of Equation 2.42 due to

$$\sigma(t) = \sigma_j H(t-\tau) + \sigma_k H(t-s) \tag{2.50c}$$

and $\bar{\epsilon}_i(t)$ denote the output of Equation 2.42 due to

$$\sigma(t) = \sigma_i H(t) \tag{2.50d}$$

Then Equation 2.49 may be written as

$$\epsilon(t) = \bar{\epsilon}_{ijo}(t) + \bar{\epsilon}_{iok}(t) + \bar{\epsilon}_{ojk}(t) - \bar{\epsilon}_i(t) - \bar{\epsilon}_j(t-\tau) - \bar{\epsilon}_k(t-s) + 6\sigma_i\sigma_j\sigma_k K_3(t, t-\tau, t-s) \tag{2.51}$$

If $\epsilon_{ijk}(t)$ is the measured response of the system then $K_3(t, t-\tau, t-s)$ may be determined by minimizing the difference between $\epsilon_{ijk}(t)$ and $\epsilon(t)$ over the set of $\{\sigma_i \sigma_j \sigma_k\}$ utilized in the tests. The expression for the determination of $K_3(t, t-\tau, t-s)$ is:

$$\sum_i \sum_j \sum_k \sigma_i \sigma_j \sigma_k \Big[\epsilon_{ijk}(t) - \bar{\epsilon}_{ijo}(t) - \bar{\epsilon}_{iok}(t) - \bar{\epsilon}_{ojk}(t) + \bar{\epsilon}_i(t) + \bar{\epsilon}_j(t-\tau) + \bar{\epsilon}_k(t-s) - 6\sigma_i\sigma_j\sigma_k K_3(t, t-\tau, t-s)\Big] = 0 \tag{2.52}$$

There does not appear to be any fixed criterion for the selection of the values of the constant stress values σ_i, σ_j and σ_k other than that th should cover the range of stress values likely to be encountered in actual

lines. Thus, at least the approximate number, if not the type, of required tests can be determined from a decision on the number of traces of the kernel functions desired.

The above number of loading programs are based on the assumption that the material response is represented exactly by a third order multiple integral representation. If the least squares method of the previous sections is used to evaluate the kernel functions then the required loading programs will depend upon the number m_1 of $\{\sigma_i\}$, the number m_2 of $\{\sigma_i \sigma_j\}$, and the number m_3 of $\{\sigma_i \sigma_j \sigma_k\}$ combinations over which the error term is minimized. If to each positive loading history there is also associated a similar negative loading history, then the results of approximately

$$2\left(m_1 + 2n m_2 + \frac{n^2 m_3}{2}\right) \tag{2.55}$$

loading programs must be known in order to characterize the material functions.

Even for the simple case of $n = 4$, $m_1 = m_2 = m_3 = 3$ Equation 2.55 indicates that 102 load histories need to be investigated. To eliminate experimental errors it would be necessary to at least duplicate each test. Consequently, the number of tests required for a relatively fine determination of the second and third order kernel functions is prohibitive. In this investigation the number of traces of kernel functions determined is necessarily small and these traces do not extend over extremely large time ranges.

III. EXPERIMENTAL INVESTIGATION

3.1 Introduction

In this investigation the material functions in the one-dimensional creep integral law were determined for low density polyethylene by carrying out a number of generalized creep tests. Some of the practical difficulties of using the Volterra-Fréchet expansion for the solution of simple stress problems and the accuracy of this formulation were evaluated by applying the creep integral law (with its experimentally determined kernel functions) to predict the strain responses due to some simple variable stress inputs, and comparing these results to the experimentally determined response.

The creep integral formulation was used rather than the relaxation formulation because the experimental difficulties associated with a creep test are considerably less than those for a relaxation test. Moreover, the one dimensional creep kernel functions obtained are related simply to the creep functions of the three-dimensional formulation (see Section 2.4). Additional two and three dimensional creep tests would provide additional information for determining these kernel functions. An analogous situation does not directly apply for the case of simple one-dimensional relaxation tests.

3.2 Material Utilized

As pointed out in the previous chapter, the number of loading programs necessary to completely characterize the creep functions is in the order of hundreds. For many materials the time required to carry out such a large

number of tests may be prohibitively large. Since in this investigation we were not concerned with any specific material, but instead were investigating the adequacy and practicality of utilizing a functional polynomial, we sought a "convenient" material. In the first place, this meant we desired a material which exhibited considerable viscoelastic response within minutes rather than days or weeks. In this way, the major portion of the viscous response could be examined in a fairly short time, and a considerable number of tests could be conducted in a limited period of time. Furthermore, since the determination of the kernel functions requires the examination of the differences of outputs due to various stress inputs, a material which exhibited a distinct nonlinear response within a short time was desirable. However, the magnitude of this nonlinearity could not be so great that a third order approximation to the constitutive law was not sufficiently accurate. It was also desired that this nonlinearity be due to the physical behavior of the material rather than due to finite deformation.

Fortunately, it was found that low density polyethylene (Allied Resinous Products brand-Resinol Type A) satisfied all of the above requirements. This material has an instantaneous Young's modulus of approximately 40,000 p.s.i., and it may be described as a "leather-like" material. The strain due to a step input stress is, after ten minutes, approximately twice as much as the quasi-instantaneous strain response, and the strain after 24 hours is approximately three times the instantaneous strain.

3.3 Loading Machines and Strain Measuring Instruments

Five dead-load lever type machines were used to apply the tensile and compressive loads (see Figs. 3 and 4). These machines had a mechanical advantage of approximately ten to one and were all calibrated prior to use. The step input loads were applied by placing weights on the loading pan, which the single lever then transferred to the specimen as a tensile or compressive load (see following section). The loads could not actually be applied instantaneously since this would have caused vibration of the loading machine and test specimen. However, it was found that by using good techniques, the full load could be built-up in less than one second and in most cases within one-half second. This time delay meant that the instantaneous behavior of the material could only be estimated. Dynamic tests should be performed to obtain a more accurate evaluation of the instantaneous response characteristics of a viscoelastic material.

Extensometers to be used with a "leather-like" material such as low-density polethylene should be of a light-lever type for which the material is not required to mechanically activate some strain measuring device. Unfortunately, in this investigation, it was necessary to use a mechanical extensometer (see Figs. 5 and 6). The extensometer used had a five inch gauge length and its end pieces were attached to the specimen at three points. The movement of these end pieces with respect to each other was measured by means of two Starett dial gauges placed on opposite sides of the specimen. The movement of the plunger of each dial also activated a

linear potentiometer. The average output of these two potentiometers was recorded on an X-Y plotter. This plotter gave a continuous record of the strain of the specimen. Thus for very short times a continuous plot was obtained for the output $e(t)$. The dial readings provided a check on this plot and were used to give a non-continuous record of the strain for large time values when the strain rate was very small.

The upper end of the extensometer, consisting of the dial gauges and potentiometers, was suspended from the frame of the lever machine by springs so that the force input to the specimen by the extensometer was almost entirely that due to the dial activating pressure and was negligible in its effect on the load on the specimen.

The polyethylene tension specimens were one-half inch diameter rods, eight inches long, threaded at each end. Small chains attached the threaded end grips to the lever machine. These chains were used to eliminate any bending effect and to produce as pure an axial tension in the specimens as possible.

3.4 Compression Testing Apparatus

Since in this investigation it was desired to examine the response of low density polyethylene to input stresses not only of tension or compression alone, but also to alternating stresses, an apparatus capable of applying compression or tension was designed. The compression rig built for this purpose (see Figs. 5 and 6) was designed for a specimen one-half inch in diameter and three and one-half inches long, with one-half inch of threads

on both ends. These dimensions gave a free length of two and one-half inches with a gauge length of two inches. The bottom end of the specimen screwed into a fixed support. The top end fitted into a one inch by three inch long steel grip which was allowed to slide freely within a fixed outside sleeve. This "slip-fit" was lubricated with a special friction reducing agent. A pan carrying constant weights was hung on a small ball bearing on the top of this upper grip. The top grip and the constant weights were attached to the lever arm of the loading machine by means of two wires and a small pulley. Appropriate loads on the loading end of the lever were applied so that the lever machine was exactly in balance under the weight of the specimen, grip and constant weights on the specimen end of the lever machine. When the bottom end of the specimen was attached to the fixed support, compression could be applied simply by removing some of the variable loads. A portion of the constant weight would then be resisted by the specimen. Conversely by adding weights to the variable load pan a tensile state of stress could be obtained in the specimen. (see Figure 7).

During the experimental program, actual experience with the compression testing apparatus utilized indicated that it performed quite satisfactorily. The reproducability of a particular compressive test was almost as good as that for any tensile test. For all of the tests performed, the results of only one compressive test were doubtful; they differed by a factor of approximately thirty percent from the results of two other tests for this load history. This one test was discarded as being erroneous.

An obvious disadvantage of this compression rig was that the short length of the specimen meant that the length changes were measured between points only one-quarter inch from the grips. This may have introduced an "end effect" error into the strain measurements.

3.5 Preparation of Test Specimens and Test Procedure

The test specimens were first threaded for one-half inch at each end. They were then heated to 120 degrees Fahrenheit for eight hours and then allowed to cool for at least three days prior to testing. The area of each specimen was obtained by measuring four diameters at three different cross-sections; one cross-section at each gauge point and one at the center of the specimen. Average diameter was used to determine the area. No specimen was of circular cross-section and a typical specimen had a minimum diameter of 0.495 inches and a maximum diameter of 0.505 inches. The desired stress was based on the original area of the specimen, and the load to be applied to the machine was dependent upon the specimen and also upon the calibration factor of the machine in use.

After inserting the specimen in the test rig and attaching the extensometer to the specimen a free time of at least two hours was allowed prior to initial loading. All of the tests were performed in a constant-temperature humidity room in which the temperature was 70 $\pm$ one degree Fahrenheit and the humidity was fifty percent.

The calibration of the linear potentiometers and X-Y plotter were checked at frequent intervals. The potentiometers were activated by two-one

and a half volt dry cell batteries, and a switching unit was used to switch from one test set-up to another. The time scale of the X-Y plotter was varied from one-half inch per second to one-fiftieth of an inch per second, depending upon the value of the strain rate. A stop watch was used to continually check the time scale of the X-Y plotter. From the continuous record of the X-Y plotter the strain response at discrete time increments was tabulated and used as a basis for the determination of the kernel functions.

Every loading program was duplicated on at least two specimens and the time steps (i.e., T in Equations 2.38, etc.) investigated thoroughly were one hundred and six hundred seconds. A time step T = 1200 seconds was also investigated, but not so thoroughly as the others.

An attempt was also made to determine the lateral contraction of three specimens under different stress inputs. A small differential transformer measuring strains to five millionths was used to measure diameter changes.

3.6 Stress Input Values Used to Determine the Kernel Functions

As we were concerned primarily with the physical nonlinearity of the material properties and not with nonlinearity introduced by the consideration of finite strains, it was necessary that the maximum value of the strain be kept sufficiently small. Preliminary tests indicated that, for the material being investigated, a step input stress of + 500 p.s.i. resulted in a strain of approximately 3.8% after two hours. Taking this as an upper limit, it was decided to use the following range of inputs to evaluate $K_1(t)$, $K_2(t,t)$ and $K_3(t,t,t)$.

$$\{\sigma_i \mid 100, 200, 300, 400, 500\} \qquad \text{p.s.i.}$$

For inputs of the form 2.32 ($\sigma(t) = \sigma_i H(t) + \sigma_j H(t-T)$) the following range of $\sigma_i \sigma_j$ combinations were investigated.

(a) For T = 100 secs.

$\{\sigma_i \sigma_j \mid$ 200 -200, 300 -300, 400 -200, 200 +200, 200 +300, 300 +200 $\}$ p.s.i.

(b) For T = 600 secs.

$\{\sigma_i \sigma_j \mid$ 100 -100, 200 -200, 300 -300, 400 -400, 500 -500, 200 +200, 300 +200, 400 -100, 400 -200, 500 -100, 400 -700 $\}$ p.s.i.

(c) For T = 1200 secs.

$\{\sigma_i \sigma_j \mid$ 500 -500, 200 -200 $\}$ p.s.i.

For inputs of the form 2.44 ($\sigma(t) = \sigma_i H(t) + \sigma_j H(t-T) + \sigma_k H(t-S)$) the following range of $\sigma_i \sigma_j \sigma_k$ combinations were investigated.

(a) T = 100, S = 200 secs.

$\{\sigma_i \sigma_j \sigma_k \mid$ 200-200+200, 200+300-300, 400-200+200, 300+200-200$\}$ p.s.i.

(b) T = 600, S = 1200 secs.

$\{\sigma_i \sigma_j \sigma_k \mid$ 400-200-200, 400-700+300, 300+200-500, 200+200-400 $\}$ p.s.i.

(c) T = 100, S = 1300 secs.

$\{\sigma_i \sigma_j \sigma_k \mid$ 200+300-500, 500-200+200, 200+200-400 $\}$ p.s.i.

Actually, the sets (b) and (c) immediately above were not used directly in the calculation of the kernel functions since sufficient data for associated two step inputs were not gathered. The outputs of these tests were, however, effectively used, in that these data were compared with the calculated outputs based on the kernel functions determined from all of the other tests (see for example, Figure 11).

3.7 Other Axial Loading Histories

By simply pouring water into a pail on the loading end of the lever machines, and then drawing this water away, variable load histories consisting of ramp loading and unloading were obtained. The actual load was recorded directly on the X-Y plotter by means of a calibrated load cell.

A many step loading history consisting of seven step loads was also investigated. A high positive step stress was followed at ten minute intervals by six negative step stress inputs so that a high compressive stress state was obtained after one hour. This loading history and the ramp loading histories are described in Figures 24, 25 and 26.

These variable load history tests were performed to be used as a basis for checking the accuracy of a truncated Volterra-Fréchet representation. The kernel functions previously found from the generalized creep tests were used in the third order theory to give the "theoretical" response due the above variable loading histories.

IV. EXPERIMENTAL RESULTS AND EVALUATION OF KERNEL FUNCTIONS

4.1 Experimental Results

Approximately eighty-five specimens (fifty tension specimens and thirty-five compression specimens) were subjected to creep tests involving one step, two step or three step stress inputs. A typical X-Y recorder plot of strain against time is shown in Figure 8. From these experimental plots the strain at various times after loading was determined. The approximate magnitude of the experimental errors was determined by comparing the results of duplicate tests. In Table 1 are presented the experimentally determined strain 600 seconds after initially applying the single step load. These results indicate that the experimental strain errors were kept below five percent except in two cases where the total strain was small. The error in strain for these cases was less than 0.00006 $\frac{in}{in}$. Similar values were found to apply to the results of two or three step loadings.

Figure 9 shows the creep strains obtained for single step histories of $\pm$300 p.s.i., and $\pm$500 p.s.i. Also shown are the results for two step stress histories of $\pm$ 300 p.s.i. followed by an additional $\pm$ 200 p.s.i. after 600 seconds. Also shown on this figure is the theoretical response for these step loadings. In this and all following figures, and in all further use in the text, "theoretical response" refers to the response calculated by using the three term integral polynomial together with the assumed kernel functions (see Sections 4.3 and 4.4) which were chosen to very closely fit the experimentally determined values for these kernel

functions. Figures 10 and 11 present the experimental results for other typical loading histories. The load histories shown in Figure 11 consist of an initial loading of $\pm$400 p.s.i. followed by an opposite loading of 700 p.s.i. taking the material into an opposite state of stress of $\mp$ 300 p.s.i. This stress level was then reduced to zero after an additional ten minutes. The difference between theoretical and actual strain response during the second load step was quite large. This was probably due to the fact that there was a large jump of 700 p.s.i. in stress - larger than the magnitude of any single step load actually used in the experiments to determine the kernel functions.

The time scales of these figures only go up to a maximum of twenty-five minutes. The actual tests were carried on for much longer times - in most cases two hours, and in two cases for twenty days. In these tests, the continued creep gave values for the rate of creep which continually decreased with time. Upon unloading, the creep recovery curves seemed to asymptotically approach zero, indicating no plastic deformation of low density polyethylene under the stress values utilized in this study.

The experimental data for these tests indicate that the material behaviour in compression is significantly different than the corresponding behaviour under tensile loading. This difference may be due to the fact that we used "engineering strain" as our measure of deformation. It is possible that by using some other deformation measure this difference in response between tension and compression could be significantly reduced.

In three creep tests at three different stress levels an attempt was made to measure the lateral contraction of the specimen. The differential transformer used for this purpose measured strains to five millionths, however, the recorded lateral strains were considerably less accurate than this. It was very difficult to obtain consistent readings on one diameter through the duration of the test. The value of Poisson's ratio for one test ranged from 0.462 to 0.493 during a ten minute creep test. The second test gave values ranging from 0.428 to 0.460 and values from 0.491 to 0.512 were obtained for the third test. No consistent variations in this ratio over the duration of the tests or for different stress levels could be observed, and these Poisson ratio values should be taken only as an indication that low density polyethylene behaves as a nearly incompressible material under uniaxial stress states.

4.2 Determination of the Creep Kernel Functions

Using the averaged values of strain from duplicate creep tests, isochronous curves similar to Figure 12 may be plotted. These curves indicate the value of the stress and the corresponding values of the strain for different times after initiation of the constant loading. Figure 12 shows that low density polyethylene exhibits a non-linear relationship between stress and strain even for low values of stress. The instantaneous behaviour cannot be obtained accurately from static creep tests, but Figure 12 would seem to indicate that the instantaneous behaviour is also nonlinear. The experimental stress-strain values at

any fixed value of time could be fitted with any order polynomial. As indicated in the previous chapter, we used a three term truncation of the Volterra-Fréchet multiple integral expansion. This is equivalent to fitting the experimental data of Figure 12 with a third order polynomial. The constants in this "best fit" theory were determined by the method of least squares. For single step inputs these constants represented $K_1(t)$, $K_2(t,t)$ and $K_3(t,t,t)$ for each fixed value of t.

For all single step loading creep tests, the maximum difference between experimental and theoretical strain values occurred at two seconds after loading at the 500 p.s.i. stress level.

For +500 p.s.i.,

e (2 sec) Experiment = 0.01727

e (2 sec) Theory = 0.01763

Difference = 0.00026

Percent difference = 1.5

For -500 p.s.i.

e (2 sec) Experiment = -0.01607

e (2 sec) Theory = -0.01646

Difference = 0.00039

Percent Difference = 2.5

A difference of approximately 0.00038 between experimental and theoretical strains also occurred throughout the creep test at -300 p.s.i. stress level (see Figure 7). The largest percentage differences (from 6

percent to 7.5 percent difference) occurred during the early times in the 100 p.s.i. loading tests. These differences between the third order theory and the experimental values are of the same order of magnitude as the probable experimental errors. This is one justification for using only a three term expansion. Considerably finer testing techniques than were used in this investigation would have to be employed before the use of a higher order Volterra-Fréchet expansion for the constitutive equation would be justified.

The isochronous curves for single step inputs were, however, also fitted with a fifth order expansion. The first kernel function remained the same as before, but there was a one hundred percent change in the second kernel function, and a fifty percent change in the third kernel function. The differences between the strains predicted by this fifth order theory and the corresponding experimental values changed sign but remained at the same order of magnitude as those associated with the third order expansion. This not only demonstrated that the values of the kernel functions were dependent on the order of the expansion used, but also indicated that the experimental data was not sufficiently accurate to warrant a higher order expansion representation.

The first order creep kernel function $K_1(t)$ is tabulated in Table II and shown diagramatically in Figure 13. In this figure the value of $K_1(t)$ has been plotted against the logarithm of $t + 1$. The instantaneous value of $K_1(t)$ could not be determined and in fact the values of all the kernel functions for the first few seconds should be viewed as suspect, since the

step loads were actually built up to their maximum values over the period of one-half to one second. The plotted points in Figure 13 are the values obtained from the experimental data, and the solid line is the value assumed for $K_1(t)$ in further calculations. It appears from Figure 13 that $K_1(t)$ might be approximated by a straight line on a log $t+1$ plot. The few tests carried out for a number of days, however, indicated that the line in Figure 13 would decrease in slope for higher time values. No attempt was made to find a closed form expression for this kernel function since numerical integration techniques were required in subsequent phases of this investigation. For this reason, $K_1(t)$ was left in a tabular form suitable for numerical integration.

4.3 Approximation of the Second Order Kernel Function

The same least-squares procedure was used in the analysis of the results of two step and three step inputs to determine values of the second and third order kernel functions for non-equal arguments.

The values obtained for the kernel functions from these tests, are probably not as accurate as those obtained for $K_1(t)$, $K_2(t,t)$ and $K_3(t,t,t)$ because there were only two or three duplicate tests carried out for each two or three step input. Furthermore, the value of the kernel functions for non-equal arguments are dependent on the differences between different tests. For example, the strain response shown in Figure 9 due to a two step input of 300 p.s.i. followed by 500 p.s.i. cannot be used directly to determine $K_2(t+T, t)$. Equation 2.41b indicates that the appropriate strains

due to a 300 p.s.i. and to a 200 p.s.i. input must be subtracted from this result in order to obtain $K_2(t+T, t)$. Experimental errors of five percent in each test could well give very large percentage errors in this difference. Fortunately, the least-squares method employs a set of inputs $\{\sigma_i \sigma_j\}$ to determine the kernel function so that the percentage error in the determined function will be less than the percentage error associated with any one group of tests within the set.

The plotted points in Figures 14, through 17, indicate the values of the second order kernel function obtained from the experimental data. The solid line indicates the assumed value of this kernel function.

To apply the theoretical constitutive equation to the solution of simple stress problems it is necessary to know the value of the second order kernel function $K_2(t_1, t_2)$ at all values of t_1 and t_2 . It was thus necessary to interpolate and extrapolate from the experimentally determined values $K_2(t,t)$, $K_2(t+100, t)$, $K_2(t+600, t)$ and $K_2(t+1200, t)$. The interpolation method applied in this case was to determine a closed form expression for $K_2(t_1, t_2)$ which fitted the experimentally determined values and then this expression was used as defining this kernel function at other time values.

An examination of the data values for $K_2(t_1, t_2)$ indicated that this function could be represented quite closely in the form

$$K_2(t_1, t_2) = f(t_2) \tag{4.1}$$

for $t_1 \geq t_2$.

The function $f(t_2)$ was chosen as a sum of exponential terms and a small correction term involving t_1 was added.

The solid lines in Figures 14 to 17 indicate the assumed values of $K_2(t_1, t_2)$ and are given by:

$$\frac{K_2(t_1, t_2)}{\left(\frac{\ln^2 10^{-3}}{16}\right)^2} = 0.0019 + 0.002116\left(1 - e^{-\frac{t_2}{10}}\right) + 0.002052\left(1 - e^{-\frac{t_2}{100}}\right) + 0.00314\left(1 - e^{-\frac{t_2}{1000}}\right) + 0.00236\left(1 - e^{-\frac{t_2}{10{,}000}}\right) + 0.0009\left(1 - e^{-\frac{t_1}{290}}\right) \qquad (4.3)$$

for $t_1 \geq t_2$ where the time is in seconds.

The above expression fits all of the values of $K_2(t_1, t_2)$ obtained from the experimental data quite closely. Since the instantaneous behavior of the material cannot be obtained from the results of the static creep tests used in this investigation, the above expression may well be in error for very small values of t_2 .

4.4 Approximation of the Third Order Kernel Function

The plotted points in Figures 18 through 23 indicate the experimentally determined values for $K_3(t_1, t_2, t_3)$. Figures 22 and 23 indicate the sensitivity of $K_3(t+600, t, t)$ and $K_3(t+600, t+600, t)$ to the sets of σ_i and σ_j stress values used to determine these functions. The values obtained for these functions certainly depends on the minimization

criteria and the set of stress values used, but the differing values shown in Figures 22 and 23 are probably due to errors in the test data.

As in the case for the second order kernel function it was desired to find a closed form expression for $K_3(t_1,t_2,t_3)$ which could either be used for direct integration of the third order integral for the solution of simple stress problems or could be used as a consistent basis for interpolation to obtain values of $K_3(t_1,t_2,t_3)$ to be used in a numerical integration procedure.

The exponential behavior of $K_3(t,t,t)$ suggested the use of an expression involving exponentials such as:

$$f(t_1,t_2,t_3) = a_0 + b_1\left(1-e^{-\frac{t_1}{c_1}}\right)\left(1-e^{-\frac{t_2}{c_1}}\right)\left(1-e^{-\frac{t_3}{c_1}}\right) + b_2\left(3-e^{-\frac{t_1+t_2}{c_2}}-e^{-\frac{t_1+t_3}{c_2}}-e^{-\frac{t_2+t_3}{c_2}}\right) \tag{4.4}$$

Nonlinear regression techniques were used with a many-term expansion similar to Equation 4.4. The results of this study indicated that $K_3(t_1,t_2,t_3)$ could not be approximated with any degree of accuracy by this type of expression. One reason for this is that the constants b_1, b_2 etc., in Equation 4.4 should be positive in order to give the exponential type of increase of $K_3(t,t,t)$. With positive values for these constants the value of $f(0,0,0)$ is then smaller than any value of $f(t,0,0)$ or $f(t_1,t_2,0)$. Figures 18 through 23 indicate that $K_3(t_1,t_2,t_3)$ does not behave in this manner. No further attempts were made to find a simple closed form expression for the third order kernel function which could be used in a

direct integration of the third integral, but rather a complicated closed form expression was found which was used for interpolation and extrapolation from the experimentally determined values of $K_3(t_1, t_2, t_3)$.

Figure 18 indicated that $K_3(t,t,t)$ might be approximated by an expression of the form

$$f(t) = a - \frac{b}{\cosh\left[c \ln(t+1)\right]} \tag{4.5}$$

Following the lead suggested by the fact that $K_2(t_1, t_2)$ could be approximated quite closely by a function of only one variable (t_2, for $t_1 \geq t_2$), the expression

$$a_1 - \frac{a_2}{\cosh\left[a_3 \ln(t_3+1)\right]} \tag{4.6}$$

was investigated as an approximation to $K_3(t_1, t_2, t_3)$ for $t_1 \geq t_2 \geq t_3$. In this expression the constant a_1 is the value approached at large values of t_3. The data indicated that the different functions $K_3(t+100, t, t)$ etc., all approached a common limit at large t values. The combination $a_1 - a_2$ in Equation 4.6 is the value of this expression for $t_3 = 0$. An examination of the data values indicated that this initial value for the various experimentally determined functions could be approximated by a function of only one variable:

$$S = t_1 + t_2 - 2t_3 \tag{4.7}$$

These considerations eventually lead to the following approximate expression for $K_3(t_1, t_2, t_3)$.

$$\frac{K_3(t_1, t_2, t_3)}{\left(\frac{in^2\ 10^{-3}}{lb}\right)^3} = 0.0435 - \left\{0.0435 - \frac{0.0235}{\cosh\{0.54 \ln(0.0623S+1)\}}\right\} \frac{1}{\cosh\left\{0.409 \ln\left[t_3(0.784e^{-0.012S} + 0.216e^{-0.00038S}) + 1\right]\right\}} \tag{4.9}$$

for $t_1 \geq t_2 \geq t_3$.

The solid lines in Figures 18 through 23 are plots of this assumed value. This expression indicates that the third order function of three variables has been expressed as a function of two variables (t_3 and $t_1 + t_2 - 2t_3$). If this were exactly true it would mean a considerable reduction in the number of tests required to completely describe this function. However, Figure 21 indicates that $K_3(t_1, t_2, t_3)$ can only be approximately described using this function.

Other interpolation techniques could have been used to evaluate $K_3(t_1, t_2, t_3)$ at values other than those experimentally determined, but the above closed form expression was used as a matter of convenience.

V. EXPERIMENTAL COMPARISON

5.1 Introduction

We used as a test of the appropriateness of the finite order integral representation, and our method of determining the kernel functions in this one dimensional constitutive equation, a comparison between the actual strain response of the material to a number of variable loading histories and the corresponding response predicted by our theory. Three variable load history tests, chosen specifically for this purpose, were performed. These tests were a load history consisting of seven step loads and two loading patterns built up of various ramp loadings and unloadings.

5.2 Multiple-Step Loading Test

Previous investigators [15,16] have demonstrated that various superposition principles encounter difficulties when trying to predict the material response due to decreasing loads. For this reason, as a relatively severe test of the third order approximation used here, it was decided to apply a multistage load history consisting of an initially high stress, decreasing in moderately large jumps. The complete load history is shown in Figure 24. An initial step stress of +450 p.s.i. was decreased to -450 p.s.i. in six steps of 150 p.s.i. The experimentally determined strain is given by the solid line and indicates the average of two tests. The dotted line indicates the contribution to the strain predicted by our third order theory due to the linear term of the third order constitutive

equation. The crosses indicate the sum of the linear and the second order terms and the circled points give our complete theoretical response. It is seen from Figure 24 that the maximum difference between the theoretical and experimental strains is 0.00105 or less than four percent. For the great majority of the time, the difference is much less than that figure.

When the time is greater than 3600 seconds, the time derivative of this input is given by

$$\dot{\sigma}(t) = 450\,\delta(t) - 150\,\delta(t-600) - 150\,\delta(t-1200) - 150\,\delta(t-1800) - 150\,\delta(t-2400) - 150\,\delta(t-3000) - 150\,\delta(t-3600) \tag{4.10}$$

From the third order constitutive equation

$$e(t) = \int_0^t K_1(t-\tau)\,\dot{\sigma}(\tau)\,d\tau + \int_0^t\int_0^t K_2(t-\tau_1, t-\tau_2)\,\dot{\sigma}(\tau_1)\,\dot{\sigma}(\tau_2)\,d\tau_1 d\tau_2 + \int_0^t\int_0^t\int_0^t K_3(t-\tau_1, t-\tau_2, t-\tau_3)\,\dot{\sigma}(\tau_1)\,\dot{\sigma}(\tau_2)\,\dot{\sigma}(\tau_3)\,d\tau_1 d\tau_2 d\tau_3 \tag{4.11}$$

it is seen that for this input the evaluation of the effect of the linear term involves seven terms, the evaluation of the second order term involves twenty-eight terms and the third order term involves sixty-three terms. These terms are not all of the same sign since the load history involves increasing and decreasing loading steps. For this reason each term must be evaluated very accurately in order to obtain reasonable accuracy in the final sum.

The agreement between the theoretical and experimental response due to this many step loading history is exceptionally good.

5.3 Ramp Loading Tests

Figures 25 and 26 describe two further variable load histories which were used to verify the theory. These loadings consisted of various forms of ramp loadings. These ramp loads were obtained by running water into and out of a pail on the loading arm of the testing machine. A load cell was used to record the actual load directly on the X-Y plotter.

Again the experimental data is presented in Figures 25 and 26 as the solid line; the contribution of the linear term is shown by the dotted line, and as before, represents only the linear portion of our "best fit" third order theory and does not represent the "best" linear fit; the contribution of the linear and the quadratic term by the crosses; and the complete third order theoretical strain response is presented by the circled points.

There is very good agreement between the experimental and theoretical values except for the unloading portion of the load history presented in Figure 27. The percentage error at the 600 second time for this experiment is approximately seven and one-half percent. At all other times the difference between experiment and theory is very small.

5.4 Summary

Although all possible variable load histories have not been studied, the load histories examined here can be viewed as severe tests of the adequacy of the third order approximation to the Volterra-Fréchet multiple integral representation. The exceptionally good agreement between the theoretical and experimental results for these few variable load histories indicates that the creep law for the viscoelastic response of low density polyethylene can be accurately described by a third order multiple integral representation.

VI. DISCUSSION AND CONCLUSIONS

A method which can be used to determine the kernel functions in a multiple integral representation of the constitutive equation of a nonlinear viscoelastic material has been presented. This method was used to determine the one-dimensional creep functions in a third order multiple integral representation for the creep of low density polyethylene. This material exhibited a considerable nonlinear creep response even within a short period of time. It was thus physically possible to conduct a large number of tests in order to determine the creep kernel functions at a sufficient number of points so that interpolation techniques could be used to adequately characterize these functions. These characterizations of the kernel functions were verified by demonstrating that the theoretical strains predicted by this representation for a number of variable load histories gave very good agreement with the experimentally determined strains. Thus it has been shown that the one-dimensional constitutive equation for a nonlinear viscoelastic material can be accurately described by a functional polynomial of third degree.

In order to determine the three-dimensional creep kernel functions for this material, additional sets of tests would have to be performed. These could include shearing creep tests which could be conducted by subjecting a thin tube of the material to torsion. Combined tension and torsion tests as well as triaxial tests, could also be conducted. A great deal of ingenuity and effort would be required in order to design the experimental equipment and to carry out all of the tests required to suitably determine the three dimensional creep kernel functions.

For certain stress analysis problems it may be desirable to have a relaxation integral formulation rather than a creep integral formulation. Inversion formulae for the one-dimensional multiple integral formulation are presented by Nakada [23]. These inversion formulae show that a finite order creep integral relation would, in general, yield an infinite order relaxation integral relation. It would be advantageous to have an algorithm for inversion of a "best-fit" finite order creep integral relation to a "best-fit" finite order relaxation integral representation.

The numerical integration of the second and third order integrals for the simple variable load histories used in this investigation to check the theoretical formulation are very tedious, and for more general load histories must be performed on a computer. Considerable storage would be required to hold all of the values of the kernel functions necessary for an accurate numerical integration of the three integrals. Special techniques should be developed so that a computer can efficiently evaluate these integrals. Given the numerical values of the kernel functions, it would appear that (with the assistance of a modern computer) one dimensional stress analysis problems may be effectively treated using a three term multiple integral representation. However, for two and three dimensional problems the difficulties are greatly compounded, and it is doubtful that, at present, general problems in this class can be treated effectively.

In this investigation special care was taken in the selection of a nonlinear viscoelastic material which would keep the experimental testing time to a minimum. In practice the stress analyst would be faced with the

problem of determining the constitutive equation applicable to the particular material being used. This material could well be one which creeps very slowly. The time necessary to conduct all of the tests required to satisfactorily describe the kernel functions in a multiple integral representation could then be prohibitively long. Although a finite multiple integral representation for the constitutive equation might accurately describe the response of this material, in many instances practical consideration might well rule out such a representation. In such cases, it would probably be more expedient to seek, within the stress ranges of interest, more specialized (albeit less accurate representations of the constitutive relations of materials of interest.

BIBLIOGRAPHY

1. Volterra, V., "Theory of Functionals and of Integral and Integro-Differential Equations," Dover Press, 1959.

2. Fréchet, M., "Sur les Functionelles Continues," Ann. Scientifiques de L'Ecole Normale sup., 3rd Series, Vol. 27, 1910, p. 193.

3. Green, A.E., Rivlin, R.S., "The Mechanics of Non-Linear Materials with Memory," Archive for Rational Mechanics and Analysis,

   Part I Vol. 1, 1957
   Part II Vol. 2, 1959 (with Spencer, A.J.M.)
   Part III Vol. 3, 1960

4. Spencer, A.J.M., and Rivlin, R.S., "Further Results in the Theory of Matrix Polynomials," Archive for Rational Mechanics and Analysis, Vol. 4, 1960, p. 214.

5. Pipkin, A.C., "Small Finite Deformations of Viscoelastic Solids," Reviews of Modern Physics, Oct. 1964, p. 1034.

6. Lifshitz, J.M., "Multiple Integral Representation of the Mechanical Behavior of Polyethylene," O.N.R. Report NR-064-450 Division of Applied Mathematics, Brown University, 1964.

7. Onaran, K. and Findley, W.N., "Combined Stress-Creep Experiments on a Nonlinear Viscoelastic Material to Determine the Kernel Functions for a Multiple Integral Representation of Creep." Transactions of the Society of Rheology, Vol. 9, No. 2, 1965, pp. 299-327.

8. Huang, H.C., and Lee, E.H., "Nonlinear Viscoelasticity for Short Time Ranges," Journal of Applied Mechanics, Vol. 33, No. 2, 1966, pp. 313-321.

9. Ward, I.M., and Onat, E.T., "Nonlinear Mechanical Behavior of Oriented Polypropylene," Journal of the Mechanics and Physics of Solids, Vol. II, 1963, p. 217.

10. Boltzmann, L., "Zur Theorie der Elastichen Nachwirkung," Annalen der Physik, No. 7, 1876, p. 624.

11. Leaderman, H., "Creep, Elastic Hysterisis, and Damping in Bakelite Under Torsion," Journal of Applied Mechanics, 1939, pp. 79A-85A.

12. Leaderman, H., "Creep and Creep Recovery in Plasticized Polyvinyl Chloride," Industrial Engineering Chemistry, V 35, 1943, p. 374.

13. Leaderman, H., "Large Longitudinal Retarded Elastic Deformation of Rubberlike Network Polymers," Transactions of the Society of Rheology,

Part I Vol. VI, 1962, pp. 361-382
Part II, "Application of a General Formulation of Nonlinear Response," Vol. III, 1963, pp. 111-123 (with McCracken, F., and Nakada, O.)

14. Leaderman, H., "Elastic and Creep Properties of Filamentous Materials," Textile Foundation, Washington, D.C., 1943.

15. Findley, W.N., and Khosla, G., "Application of the Superposition Principle and Theories of Mechanical Equation of State, Strain, and Time Hardening to Creep of Plastics under Changing Loads," Journal of Applied Physics, Vol. 26, No. 7, 1955, p. 821.

16. Ross, A.D., "Creep of Concrete Under Variable Stress," Journal of the American Concrete Institute, V. 29, No. 9, 1958, p. 739.

17. Wang, T.T. and Onat, E.T., "Non-Linear Mechanical Behavior of 1100 Aluminum at 300° F.," O.N.R. Report 562 (2) NR-064-424 Tech. Report 40, Brown University, 1965.

18. Evans, R.J., "Constitutive Equations for a Class of Nonlinear-Elastic Solids," Doctoral Dissertation, Univ. of Calif., 1965.

19. Lockett, F.J., "Creep and Stress-Relaxation Experiments for Non-Linear Materials," International Journal of Engineering Science, Vol. 3, 1965, pp. 59-75.

20. Brilliant, M.B., "Theory of the Analysis of Non-Linear Systems," Mass. Inst. of Tech., Research Laboratory of Electronics, March 1958.

21. George, D.A., "Continuous Non-Linear Systems," Tech. Report 355. Mass. Inst. of Tech., Research Laboratory of Electronics, July 1959.

22. Schetzen, M., "Measurement of the Kernels of a Non-Linear System of Finite Order," Mass. Inst. of Tech., Quarterly Progress Report No. 71, Research Laboratory of Electronics, Oct. 1963.

23. Nakada, O., "Theory of Non-Linear Responses," Journal of the Physical Society of Japan, Vol. 15, No. 12, 1960.

TABLE 1

Creep Strains After 600 Seconds at Constant Stress Level

Stress Value (p.s.i.)	Number of Tests	Average Strain (Percent)	Maximum Strain (Percent)	Minimum Strain (Percent)	Maximum Difference from Average	Maximum Difference {Percent of Average Strain}
100	6	0.5062	0.532	0.462	-0.0442	8.7
-100	4	-0.484	-0.50	-0.471	0.016	3.3
200	7	1.0976	1.156	1.053	0.0594	5.4
-200	7	-1.043	-1.092	-1.013	-0.049	4.7
300	5	1.744	1.795	1.704	0.051	2.9
-300	4	-1.637	-1.704	-1.577	-0.067	4.1
400	6	2.486	2.590	2.396	0.104	4.2
-400	6	-2.204	-2.295	-2.110	-0.094	4.3
500	5	3.325	3.482	3.210	0.157	4.7
-500	5	-2.889	-2.950	-2.777	-0.112	3.9

TABLE II

Experimentally Determined Value of the Linear Creep Kernel Function

Time (Secs)	$K_1(t)$ $\frac{in^2}{lb} 10^{-4}$	Time (Secs)	$K_1(t)$ $\frac{in^2}{lb} 10^{-4}$	Time (Secs)	$K_1(t)$ $\frac{in^2}{lb} 10^{-4}$
1	0.2591	55	0.4120	650	0.5237
2	0.2771	60	0.4158	700	0.5275
3	0.2908	65	0.4196	800	0.5231
4	0.3011	70	0.4232	900	0.5380
5	0.3095	80	0.4295	1000	0.5427
6	0.3162	90	0.4347	1200	0.5508
7	0.3222	100	0.4396	1400	0.5574
8	0.3275	110	0.4441	1600	0.5636
9	0.3322	120	0.4485	1800	0.5687
10	0.3367	140	0.4558	2000	0.5730
12	0.3441	160	0.4616	2500	0.5825
14	0.3508	180	0.4671	3000	0.5900
16	0,3566	200	0.4720	3500	0.5961
18	0,3615	230	0.4783	4000	0.6014
20	0.3665	260	0.4837	4500	0.606
23	0.3727	300	0.4905	5000	0.6096
26	0.3781	350	0.4970	5500	0.6137
30	0.3846	400	0.5032	6000	0.6166
35	0.3915	450	0.5084	7000	0.6230
40	0.3974	500	0.5130	8000	0.6278
45	0.4026	550	0.5172	9000	0.6317
50	0.4076	600	0.5209		

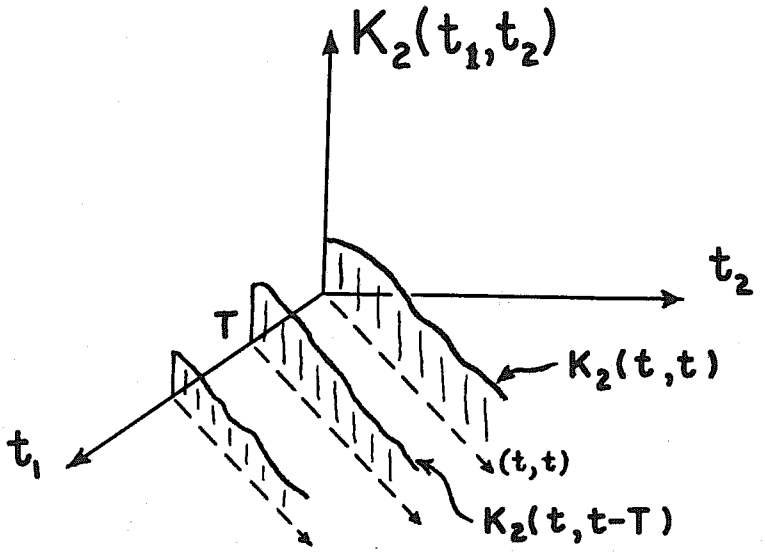

Fig. 1

Lines in the t_1, t_2 plane along which $K_2(t_1, t_2)$ is determined

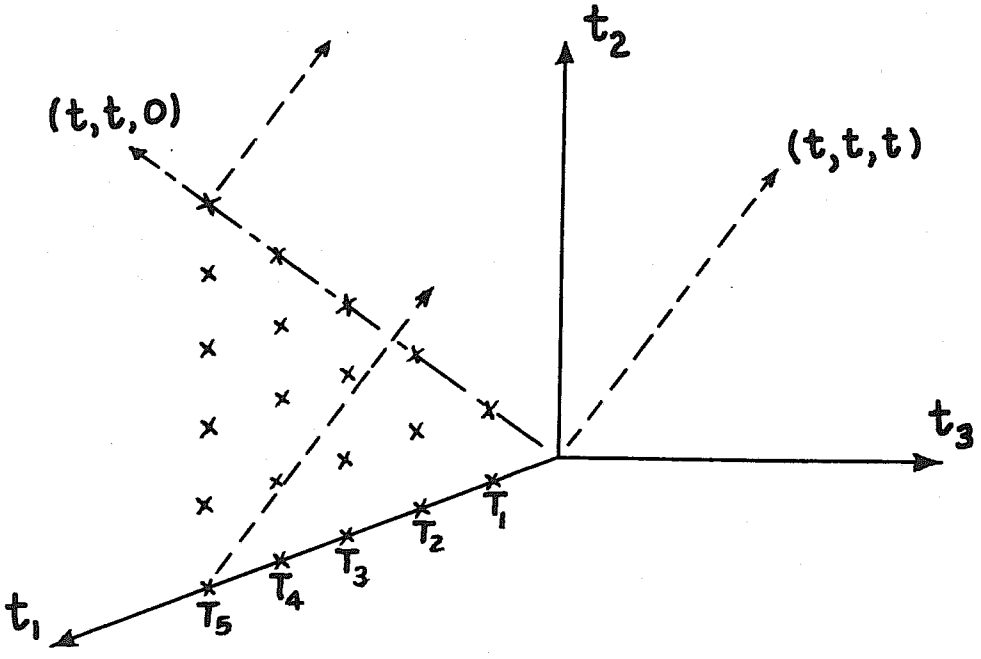

Fig. 2

Lines in t_1 t_2 t_3 space along which $K_3(t_1, t_2, t_3)$ is determined

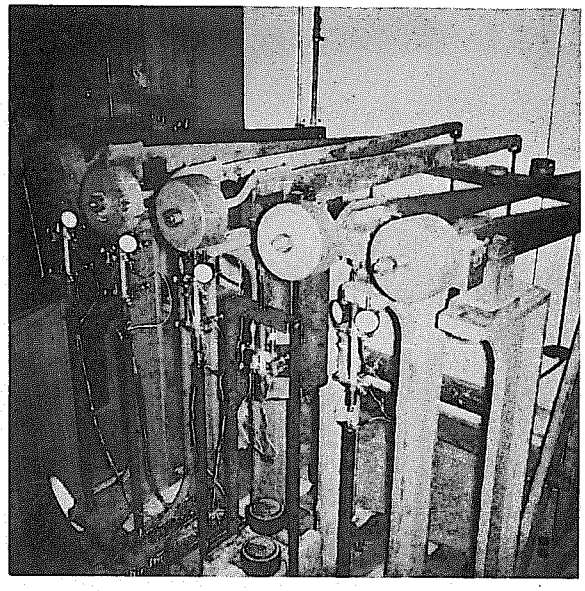

Fig. 3

General View of Loading Frames

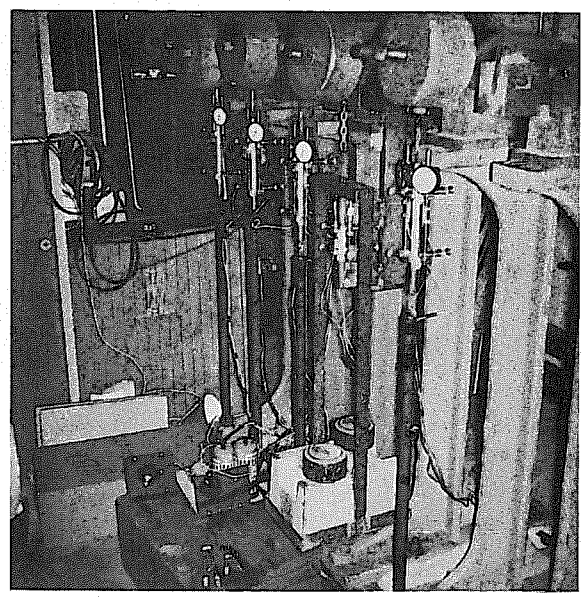

Fig. 4

General View of Test Set-Up

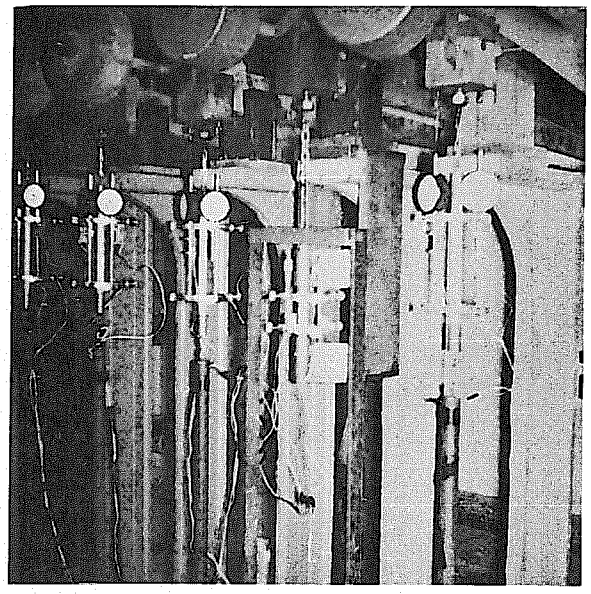

Fig. 5

Tension Specimens and Compression Testing Device

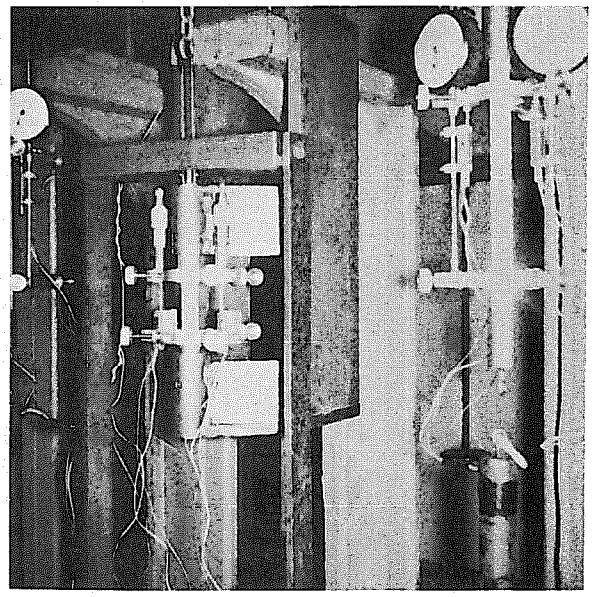

Fig. 6

Tension Specimen and Close-Up of
Compression Test Set-Up

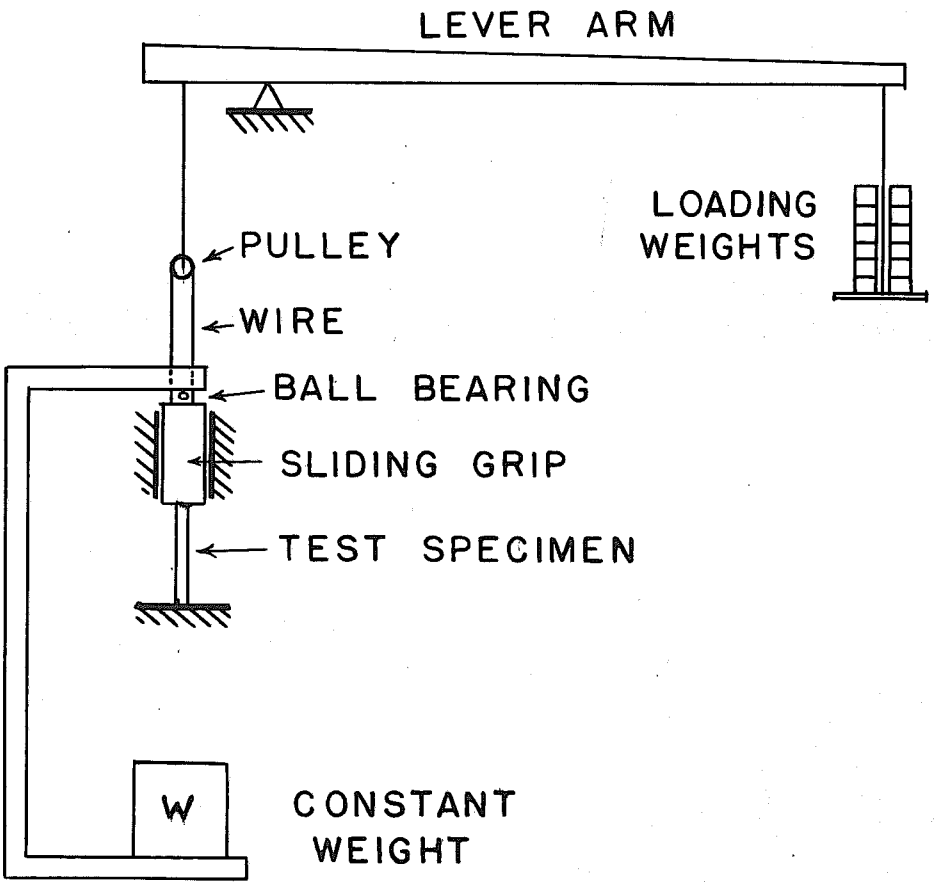

FIG. 7

SCHEMATIC DIAGRAM OF THE COMPRESSION TEST APPARATUS

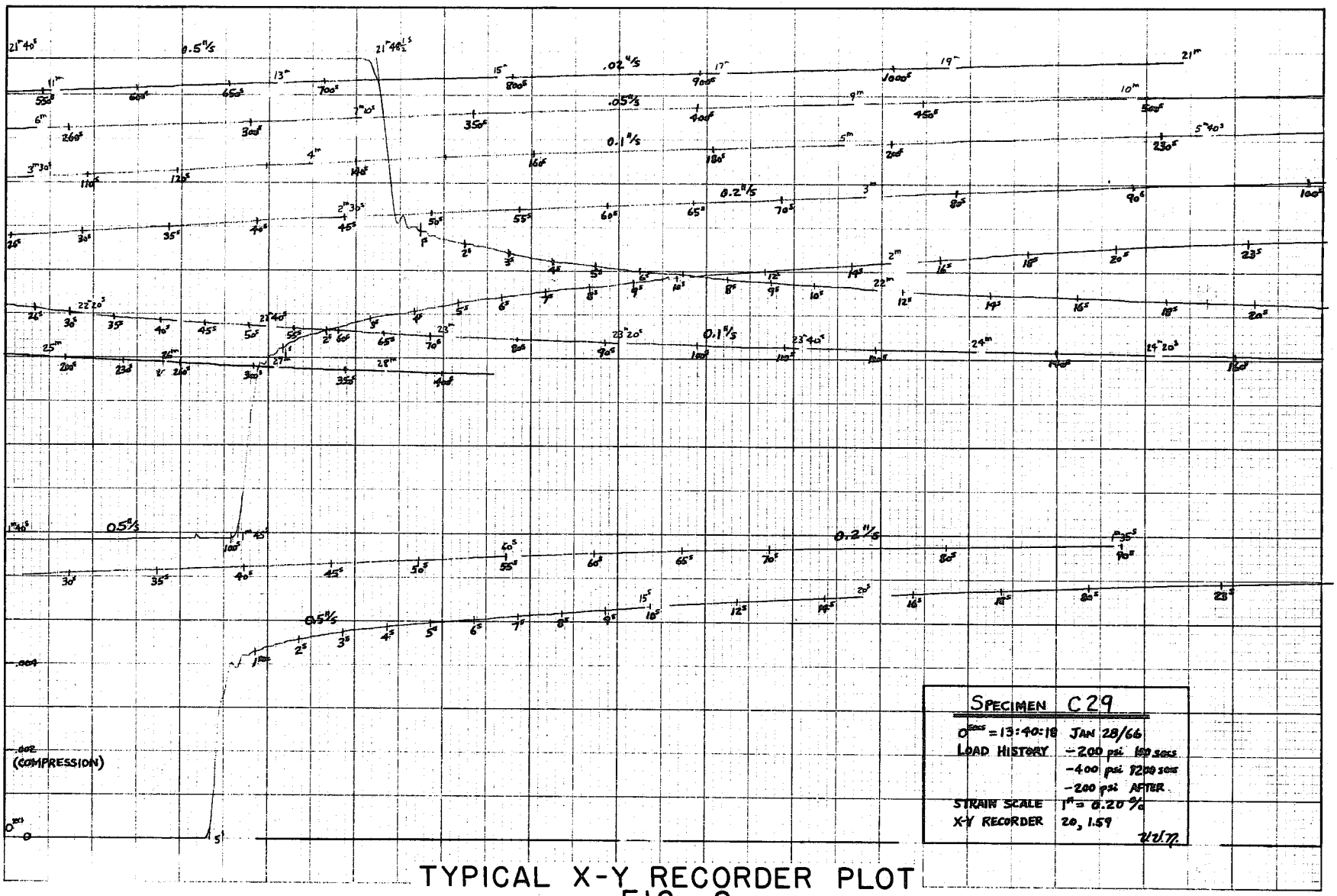

TYPICAL X-Y RECORDER PLOT
FIG. 8

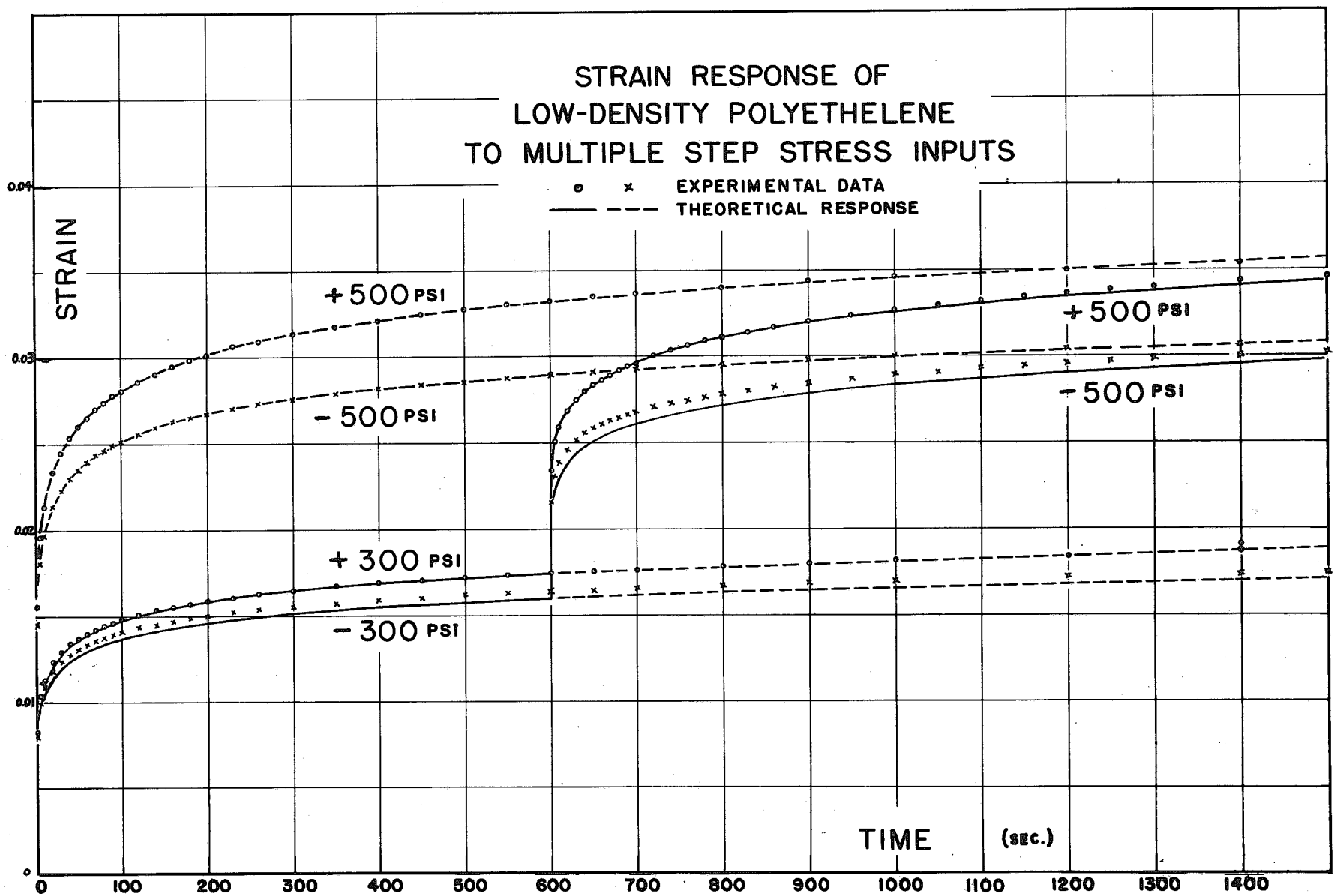
STRAIN RESPONSE OF
LOW-DENSITY POLYETHELENE
TO MULTIPLE STEP STRESS INPUTS
EXPERIMENTAL DATA
THEORETICAL RESPONSE
STRAIN
+500 PSI
-500 PSI
+300 PSI
-300 PSI
+500 PSI
-500 PSI
0.04
0.03
0.02
0.01
0
0
100
200
300
400
500
600
700
800
900
1000
1100
1200
1300
1400
TIME (SEC.)

FIG. 9

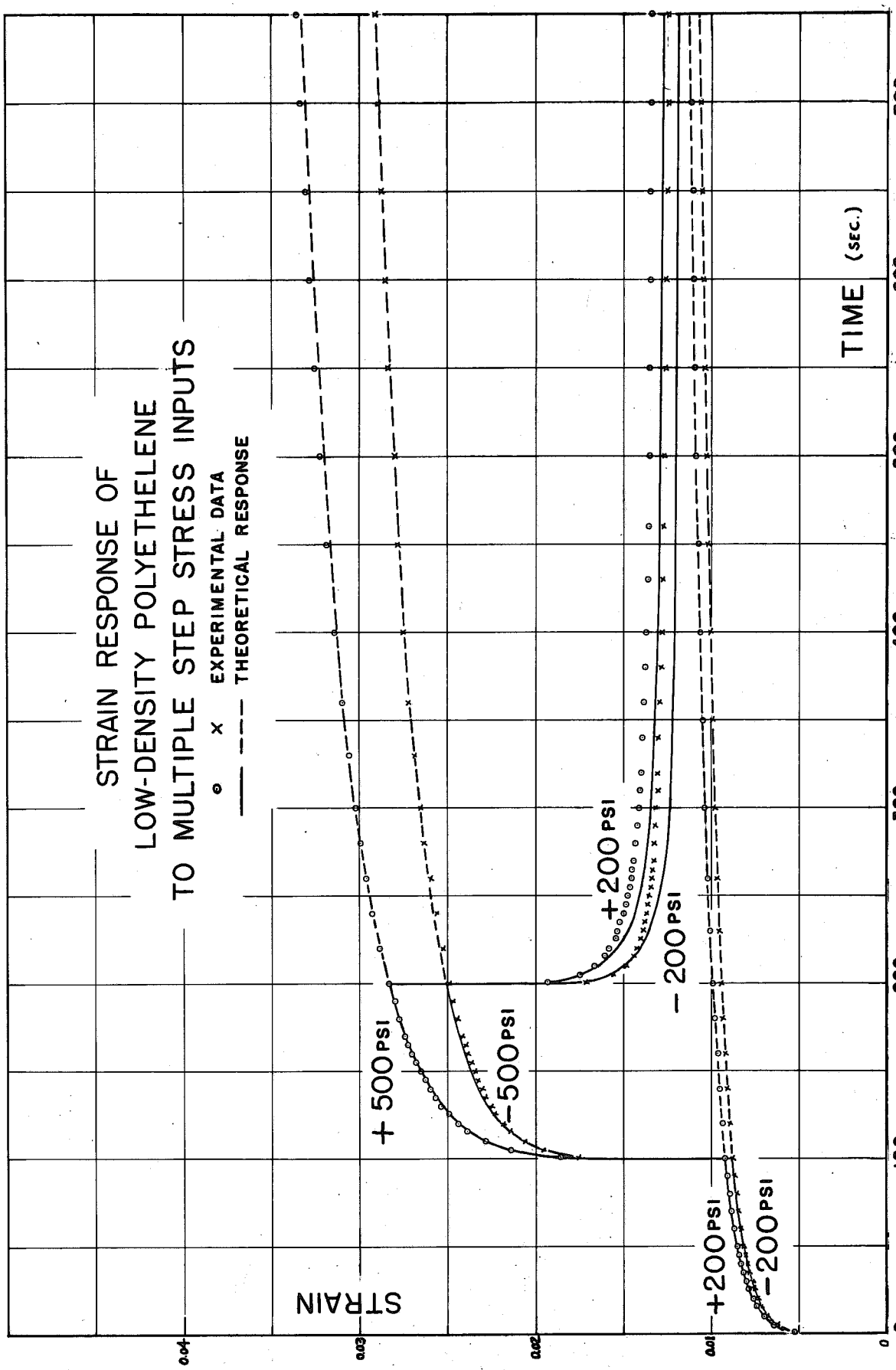
STRAIN RESPONSE OF
LOW-DENSITY POLYETHELENE
TO MULTIPLE STEP STRESS INPUTS
o x EXPERIMENTAL DATA
—— --- THEORETICAL RESPONSE
STRAIN
TIME (SEC.)
+500PSI
-500PSI
+200PSI
-200PSI
+200PSI
-200PSI
0.04
0.03
0.02
0.01
0
0
100
200
300
400
500
600
700

FIG. 10

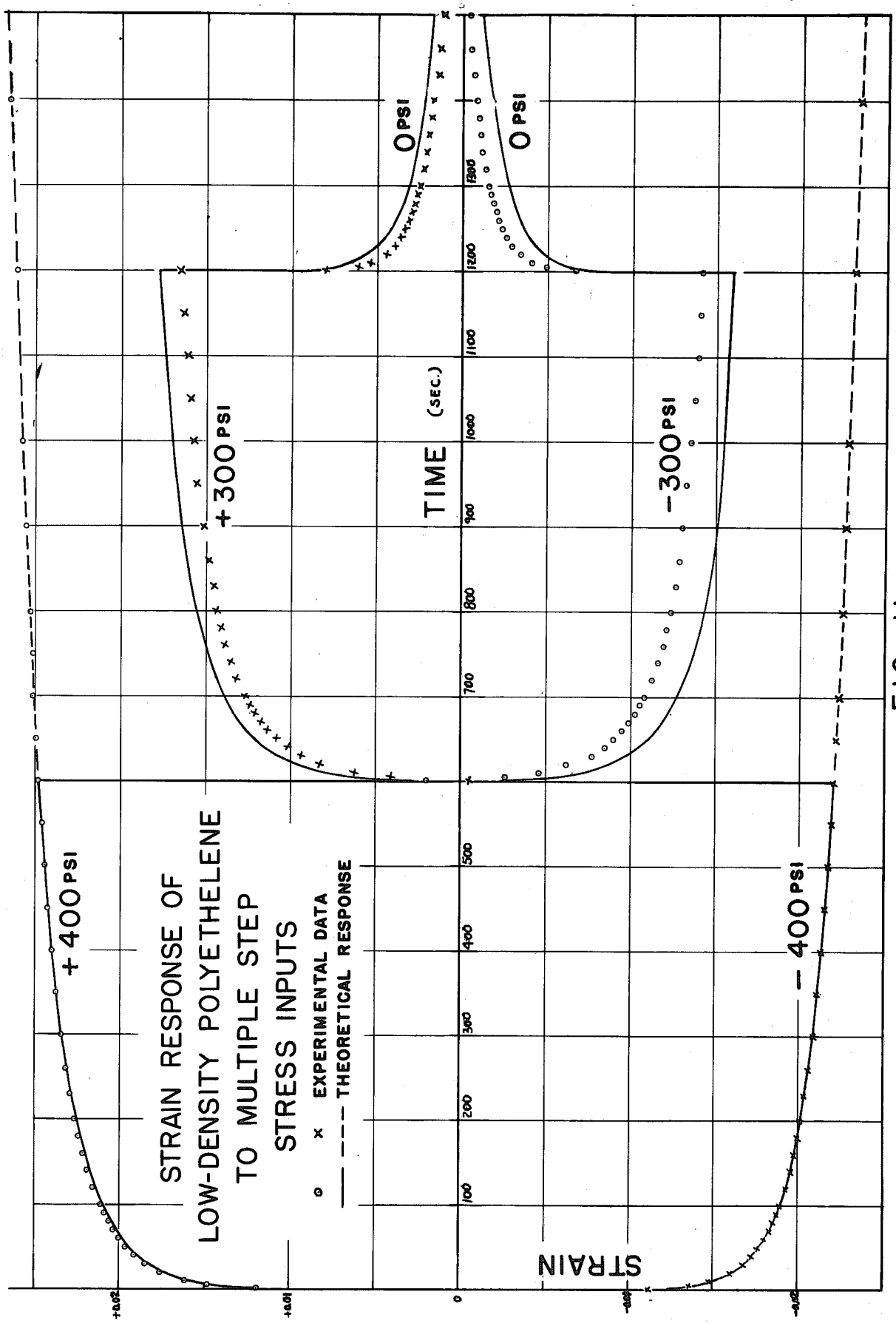
STRAIN RESPONSE OF
LOW-DENSITY POLYETHELENE
TO MULTIPLE STEP
STRESS INPUTS
o x EXPERIMENTAL DATA
— — — THEORETICAL RESPONSE
+400 PSI
+300 PSI
0 PSI
0 PSI
-300 PSI
-400 PSI
TIME (SEC.)
STRAIN
+0.02
+0.01
0
-0.01
-0.02
100
200
300
400
500
700
800
900
1000
1100
1200
1300

FIG. 11

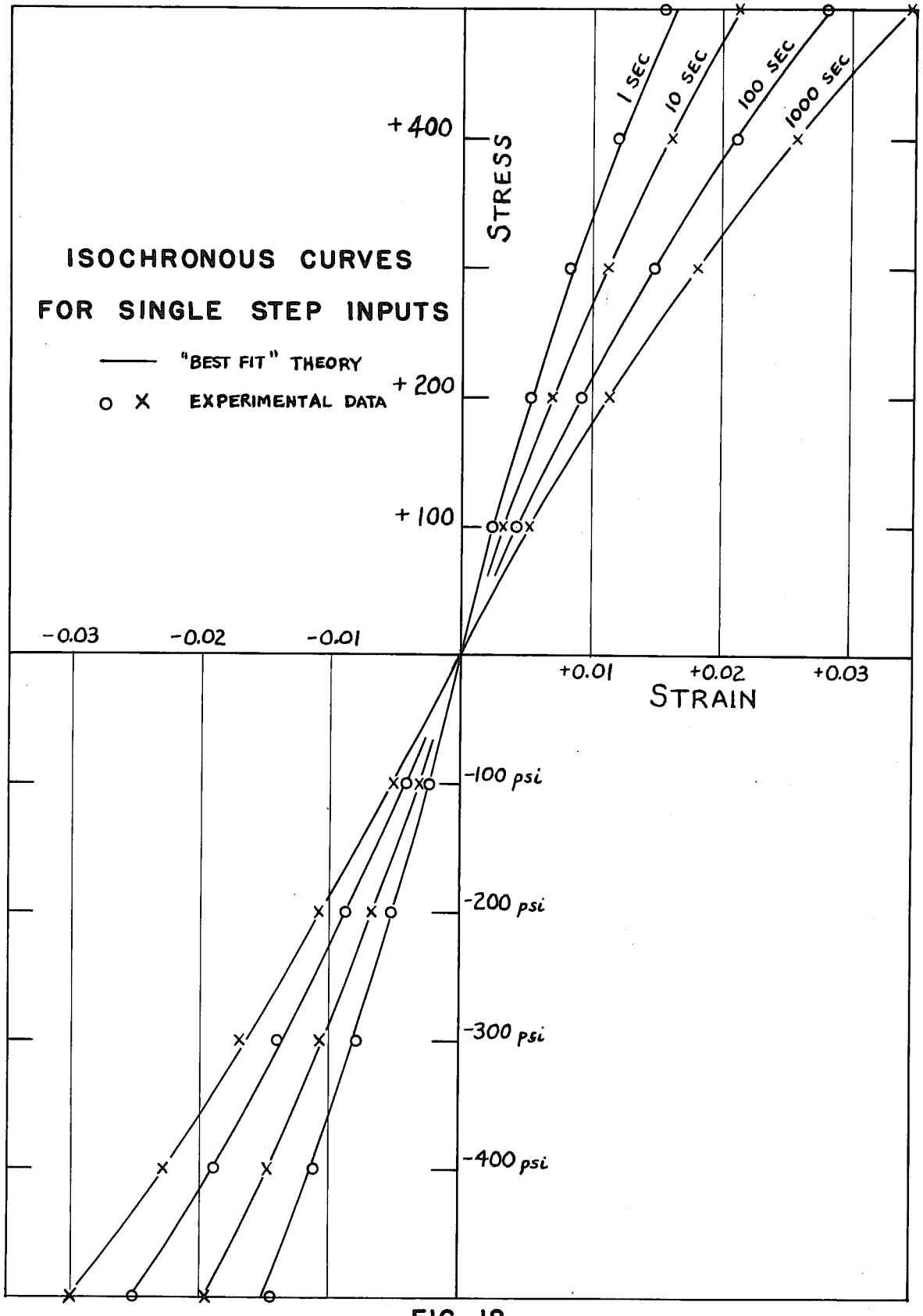
ISOCHRONOUS CURVES
FOR SINGLE STEP INPUTS
"BEST FIT" THEORY
EXPERIMENTAL DATA
STRESS
STRAIN
+400
+200
+100
-100 psi
-200 psi
-300 psi
-400 psi
-0.03
-0.02
-0.01
+0.01
+0.02
+0.03
1 SEC
10 SEC
100 SEC
1000 SEC

FIG. 12

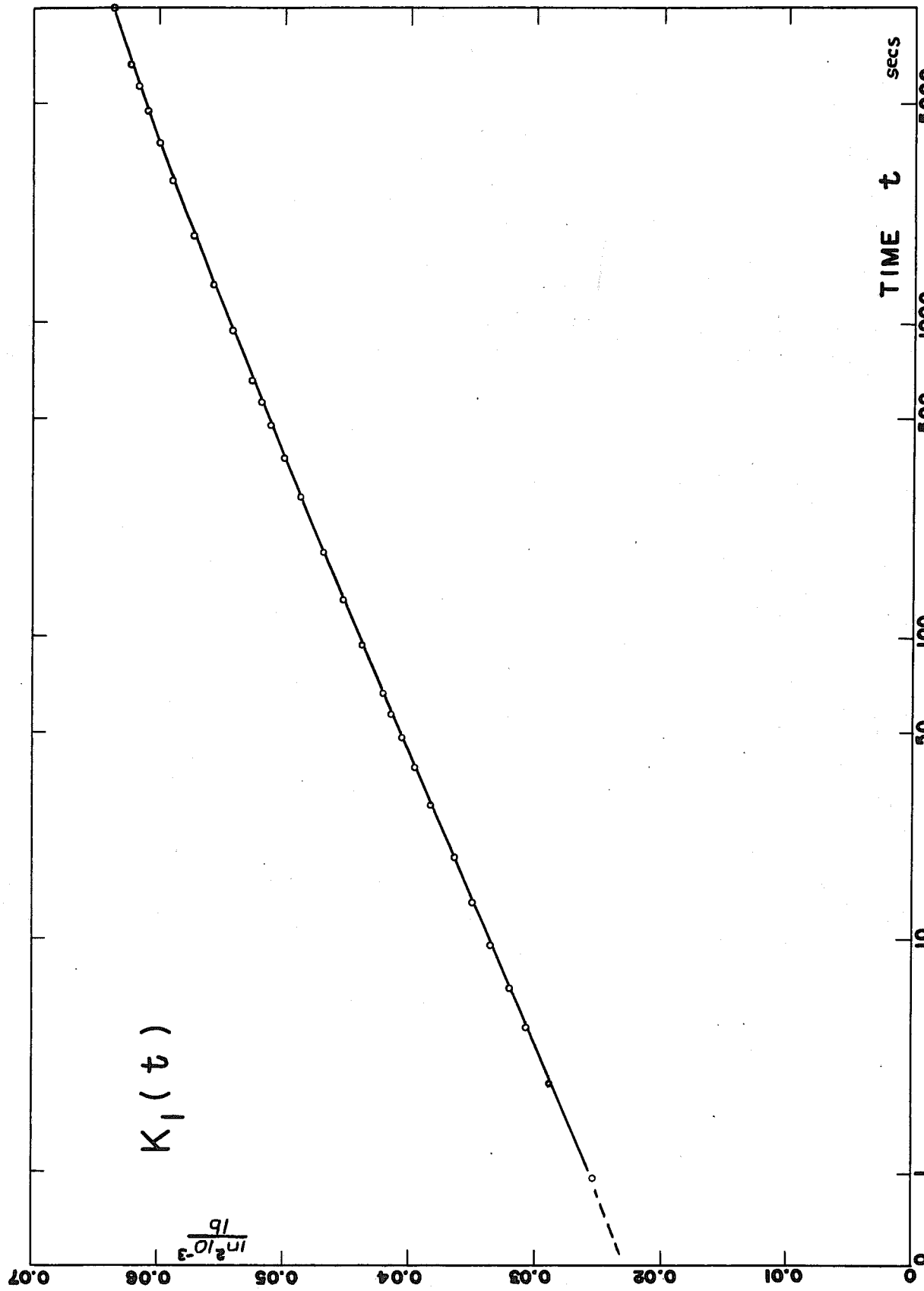
$K_1(t)$
$\frac{\ln^2 10^{-3}}{lb}$
0.07
0.06
0.05
0.04
0.03
0.02
0.01
0
TIME t secs
0
1
10
50
100
500
1000
5000

FIG. 13

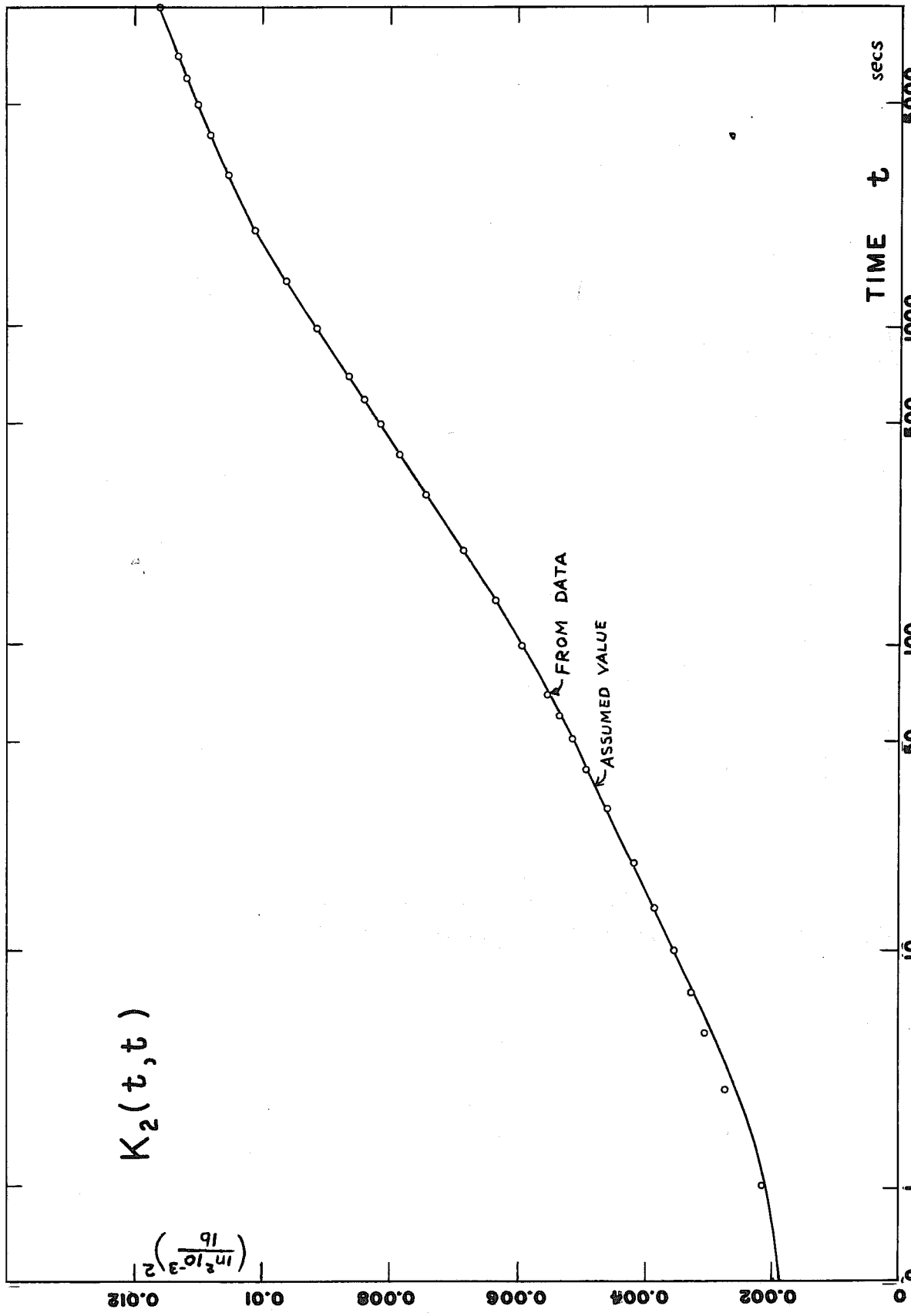
$K_2(t,t)$
$\left(\frac{in^2 10^{-3}}{16}\right)^2$
0.012
0.01
0.008
0.006
0.004
0.002
0
0
1
10
50
100
500
1000
5000
TIME t secs
FROM DATA
ASSUMED VALUE

FIG. 14

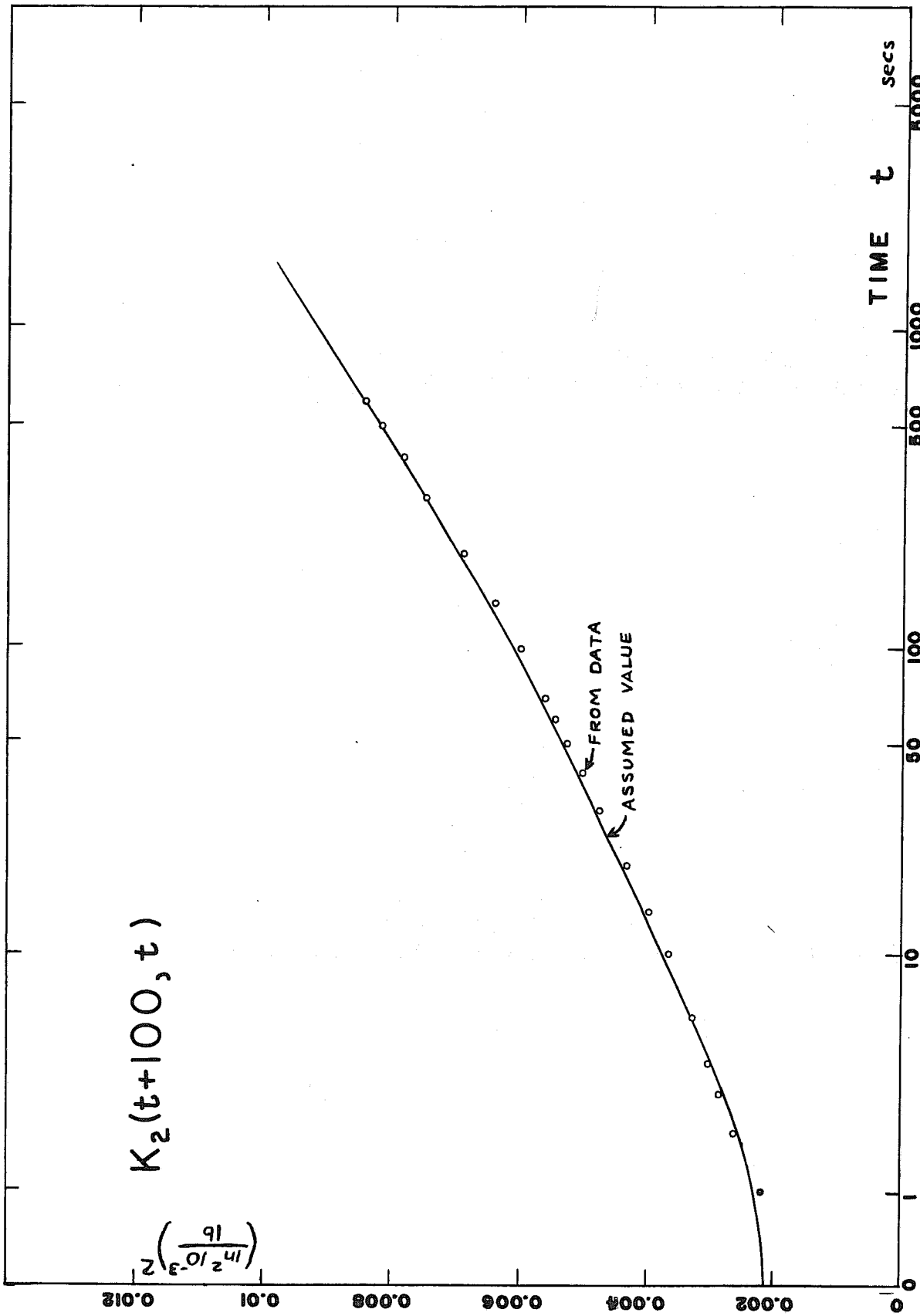
$K_2(t+100,t)$
$\left(\frac{in^2 10^{-3}}{16}\right)^2$
0.012
0.01
0.008
0.006
0.004
0.002
0
TIME t secs
0
1
10
50
100
500
1000
5000
FROM DATA
ASSUMED VALUE

FIG. 15

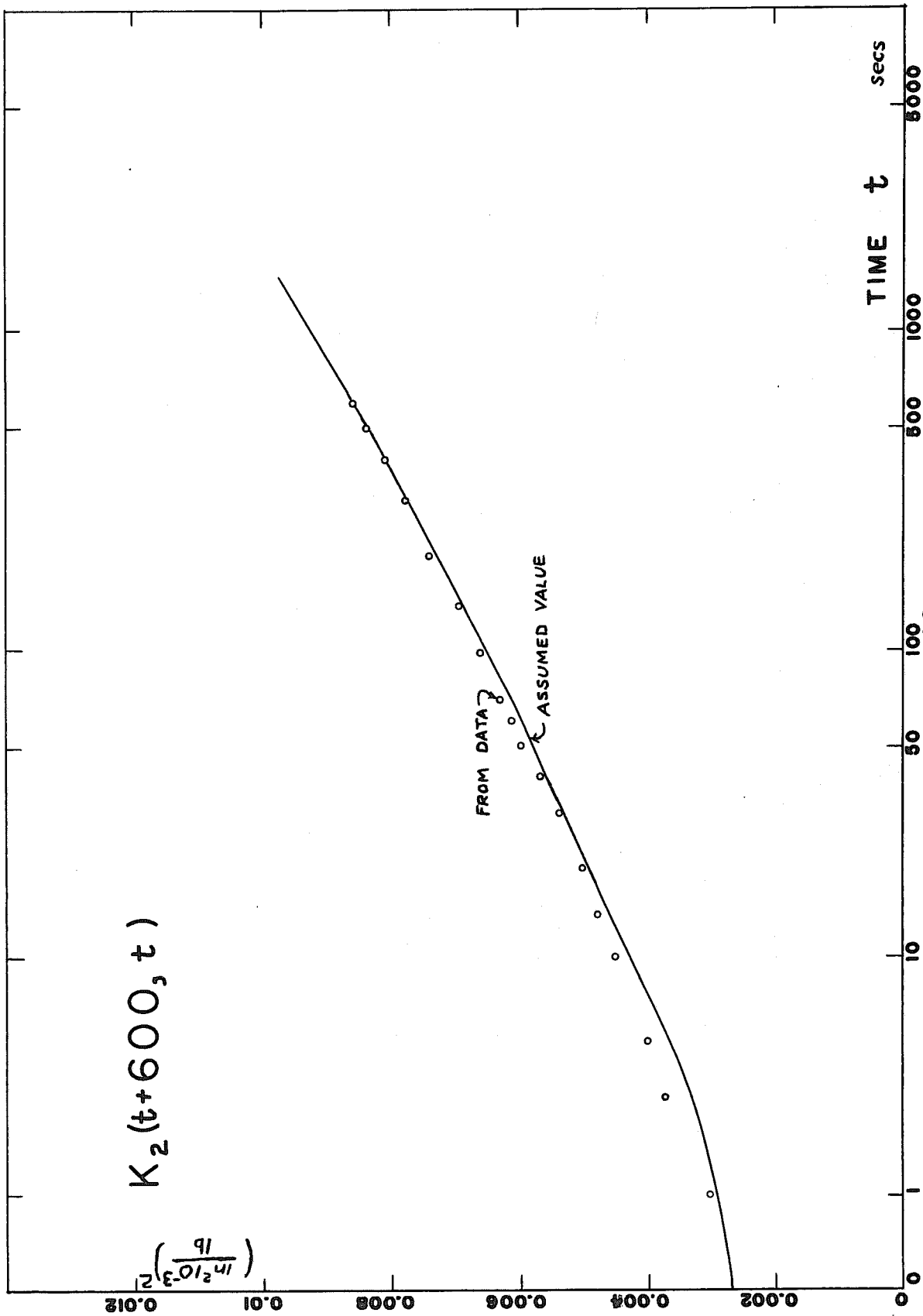
$K_2(t+600, t)$
$\left(\frac{in^2 10^{-3}}{16}\right)^2$
0.012
0.01
0.008
0.006
0.004
0.002
0
0
1
10
50
100
500
1000
5000
TIME t secs
FROM DATA
ASSUMED VALUE

FIG. 16

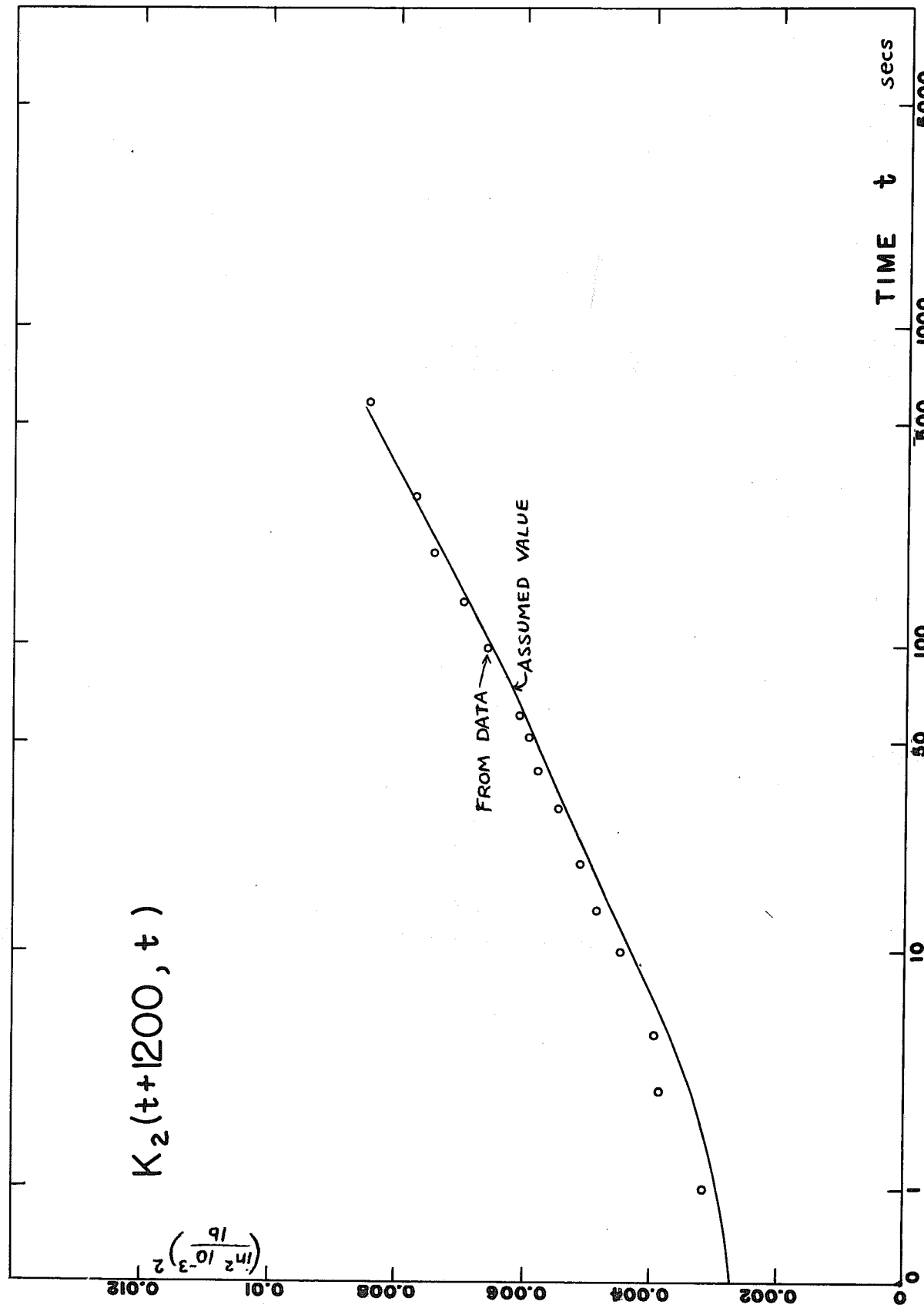
$K_2(t+1200, t)$
$\left(\frac{in^2\ 10^{-3}}{16}\right)^2$
0.012
0.01
0.008
0.006
0.004
0.002
0
0
1
10
50
100
500
1000
5000
TIME t secs
FROM DATA
ASSUMED VALUE

FIG. 17

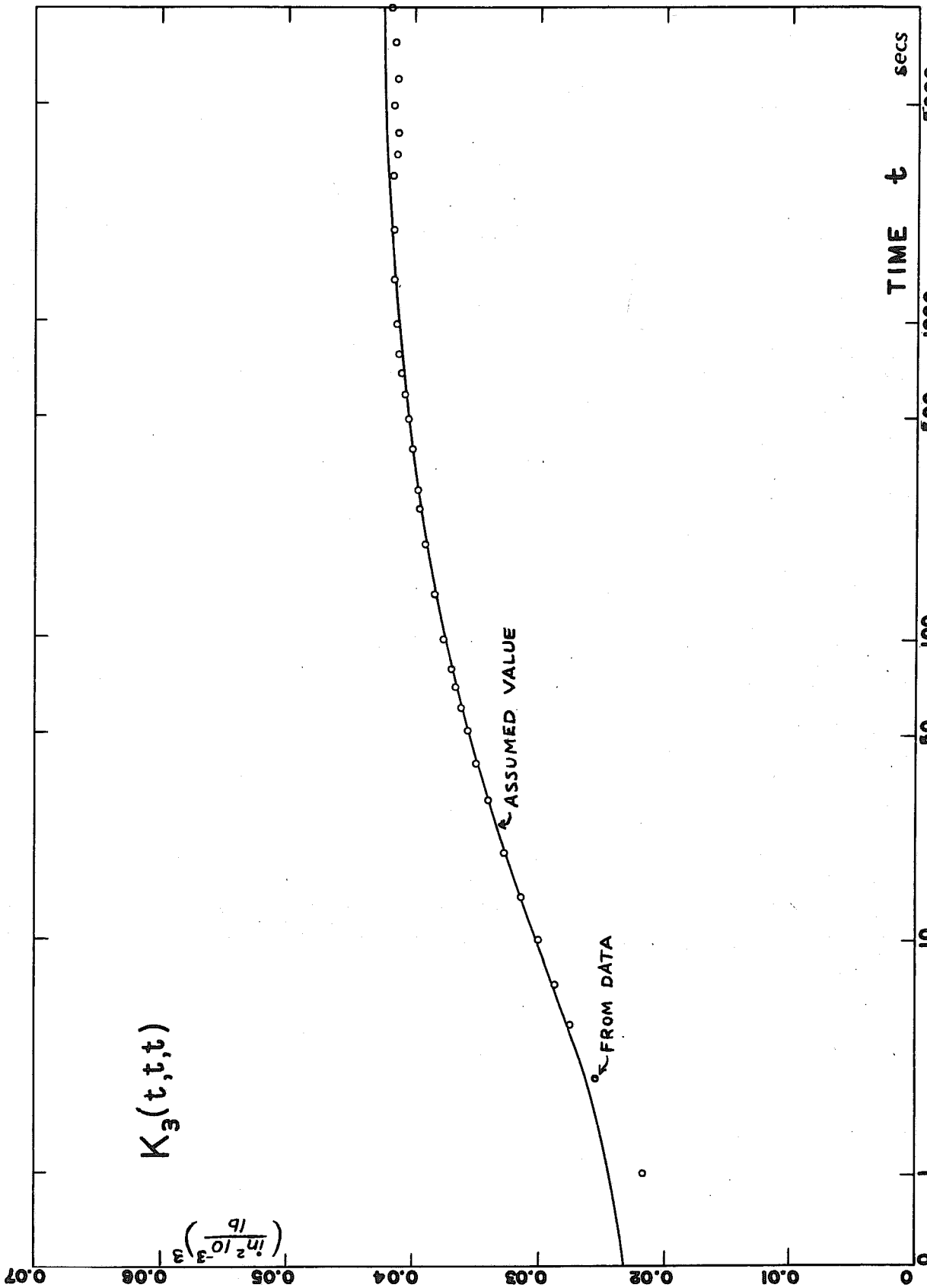
$K_3(t,t,t)$
$\left(\frac{in^2\,10^{-3}}{lb}\right)^3$
0.07
0.06
0.05
0.04
0.03
0.02
0.01
0
0
1
10
50
100
500
1000
5000
TIME t secs
ASSUMED VALUE
FROM DATA

FIG. 18

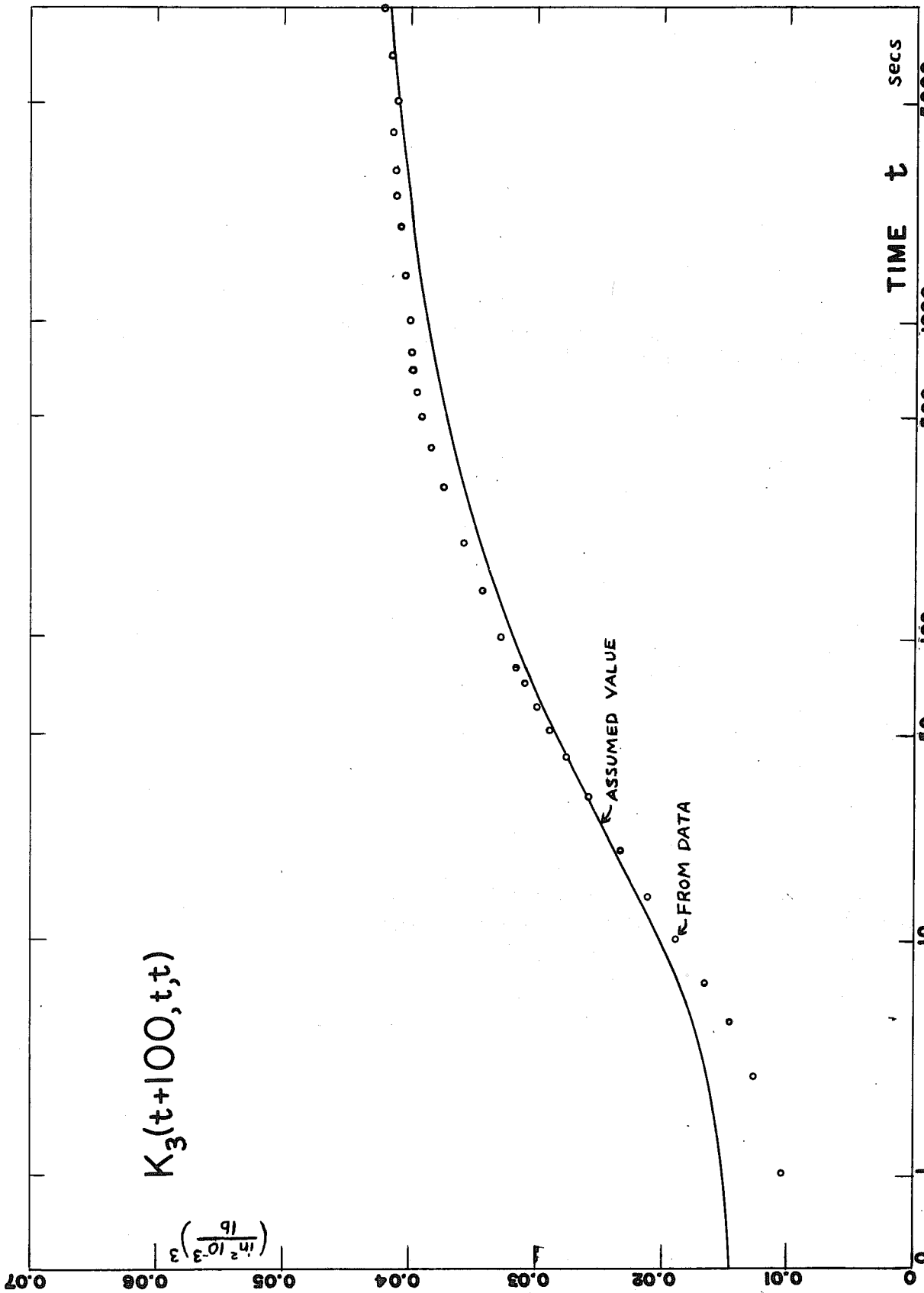
$K_3(t+100,t,t)$
$\left(\frac{in^2\,10^{-3}}{lb}\right)^3$
0.07
0.06
0.05
0.04
0.03
0.02
0.01
0
TIME t secs
0
1
10
50
100
500
1000
5000
ASSUMED VALUE
FROM DATA

FIG. 19

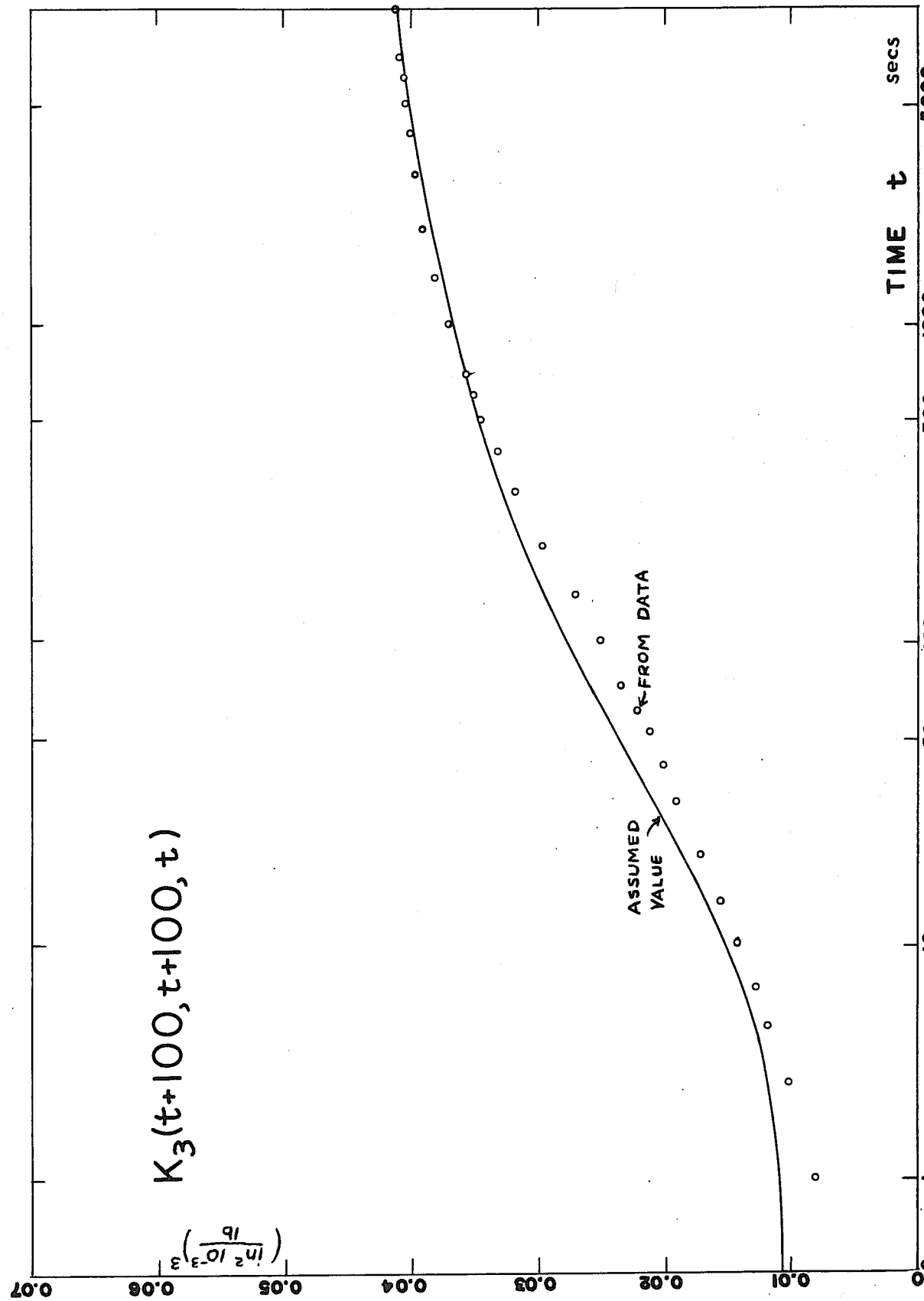
$K_3(t+100, t+100, t)$
$\left(\frac{in^2\ 10^{-3}}{lb}\right)^3$
0.07
0.06
0.05
0.04
0.03
0.02
0.01
0
ASSUMED VALUE
FROM DATA
0
1
10
50
100
500
1000
5000
TIME t secs

FIG. 20

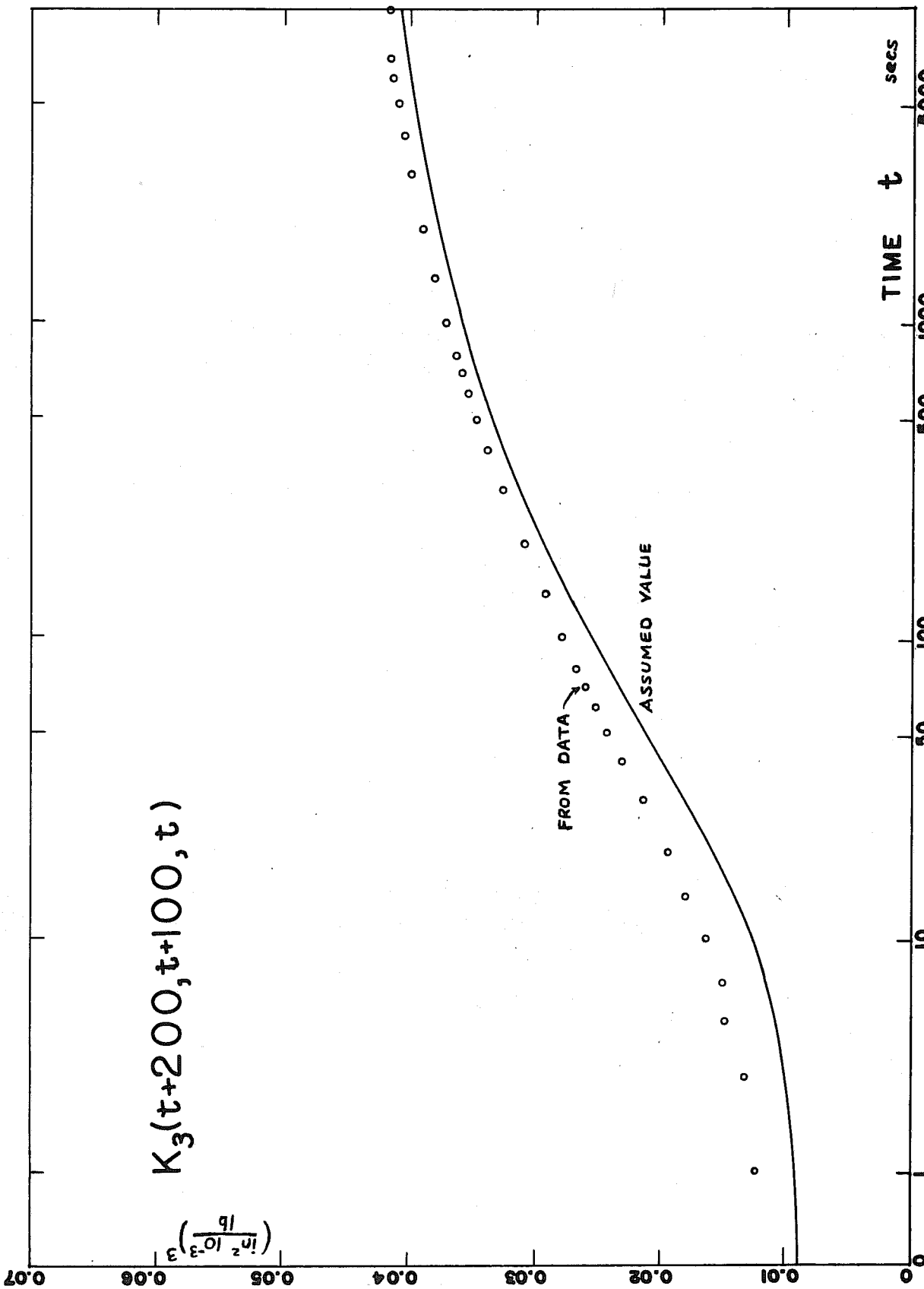
$K_3(t+200, t+100, t)$
$\left(\frac{in^2\ 10^{-3}}{lb}\right)^3$
0.07
0.06
0.05
0.04
0.03
0.02
0.01
0
FROM DATA
ASSUMED VALUE
TIME t secs
0
1
10
50
100
500
1000
5000

FIG. 21

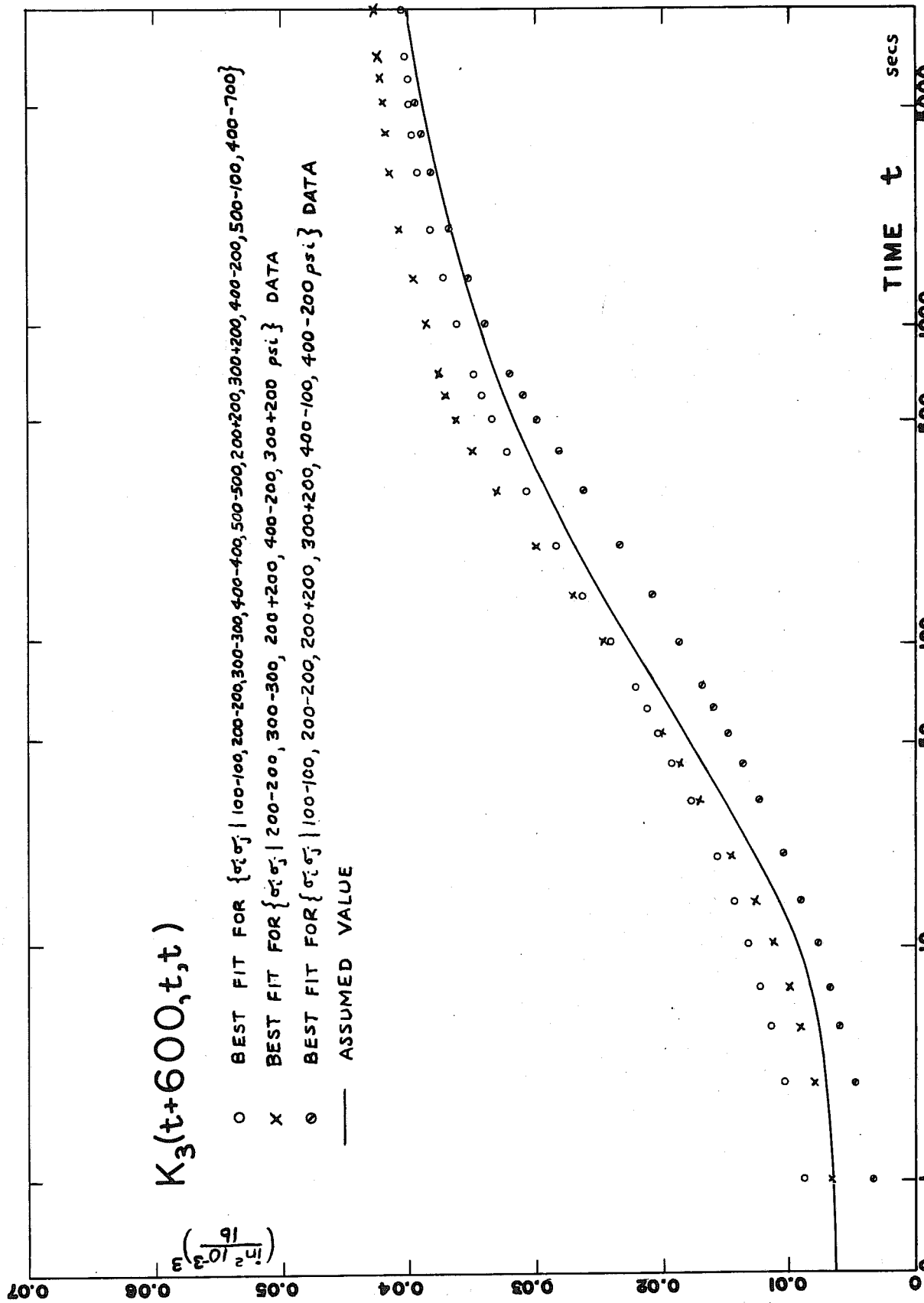
$K_3(t+600,t,t)$
$\left(\frac{in^2}{lb}10^{-3}\right)^3$
0.07
0.06
0.05
0.04
0.03
0.02
0.01
0
0 BEST FIT FOR {σi σj | 100-100, 200-200, 300-300, 400-400, 500-500, 200+200, 300+200, 400-200, 500-100, 400-700}
X BEST FIT FOR {σi σj | 200-200, 300-300, 200+200, 400-200, 300+200 psi} DATA
⊗ BEST FIT FOR {σi σj | 100-100, 200-200, 200+200, 300+200, 400-100, 400-200 psi} DATA
— ASSUMED VALUE
0
1
10
50
100
500
1000
5000
TIME t secs

FIG. 22

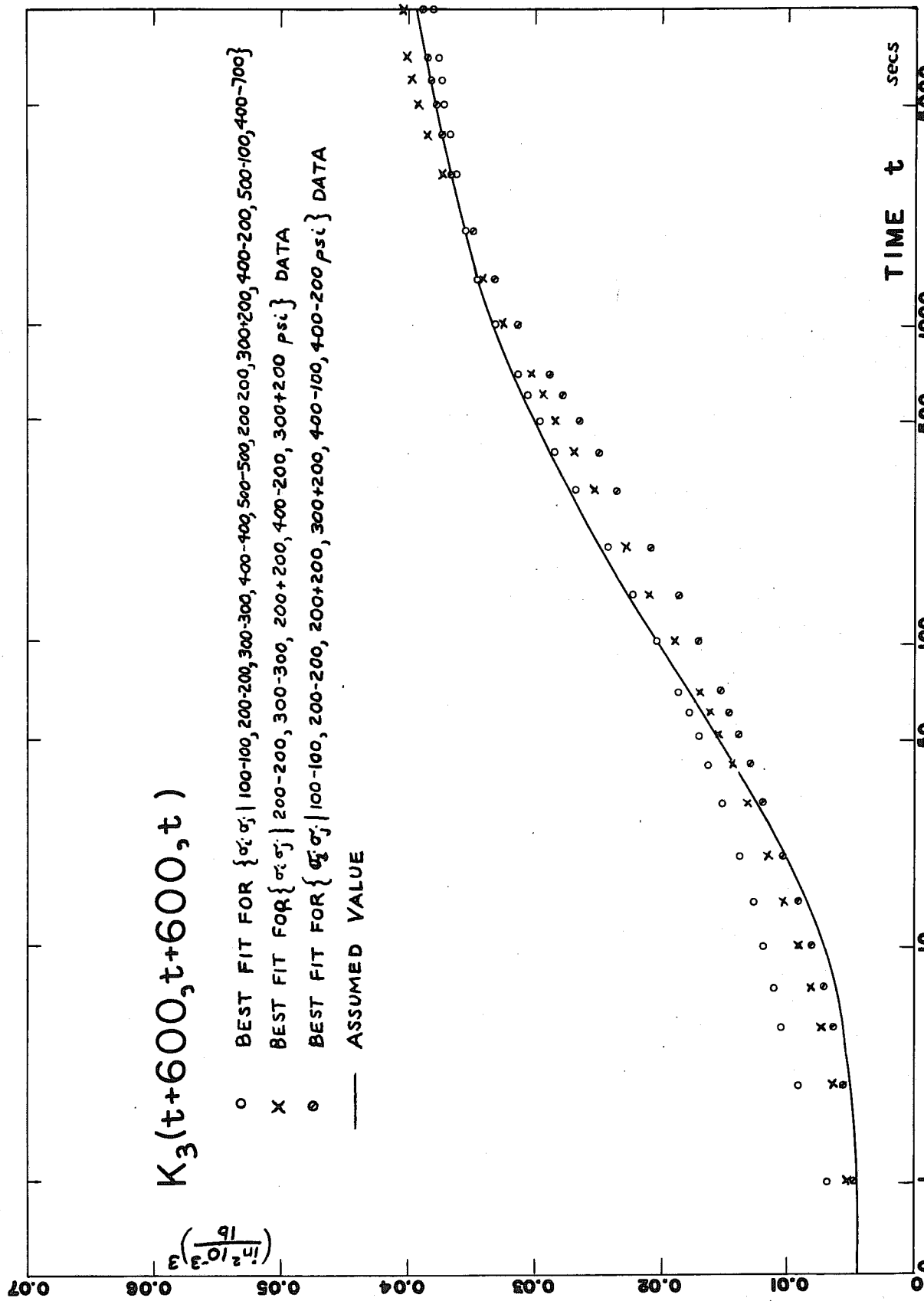
$K_3(t+600, t+600, t)$
$\left(\frac{in^2 10^{-3}}{lb}\right)^3$
0.07
0.06
0.05
0.04
0.03
0.02
0.01
0
0 BEST FIT FOR {σ_i σ_j | 100-100, 200-200, 300-300, 400-400, 500-500, 200 200, 300+200, 400-200, 500-100, 400-700} DATA
X BEST FIT FOR {σ_i σ_j | 200-200, 300-300, 200+200, 400-200, 300+200 psi} DATA
⊗ BEST FIT FOR {σ_i σ_j | 100-100, 200-200, 200+200, 300+200, 400-100, 400-200 psi} DATA
— ASSUMED VALUE
0
1
10
50
100
600
1000
6000
TIME t secs

FIG. 23

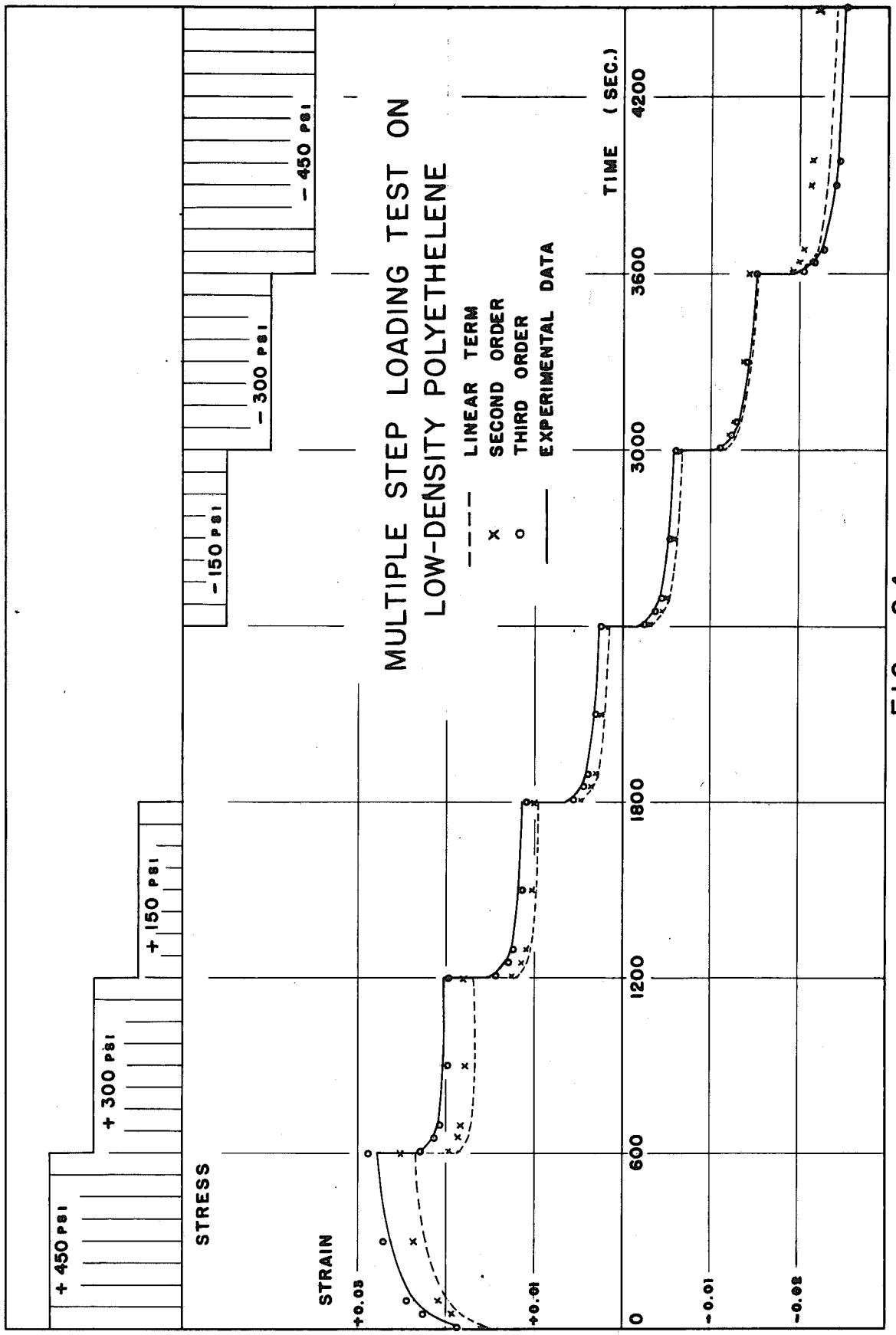
MULTIPLE STEP LOADING TEST ON
LOW-DENSITY POLYETHELENE
LINEAR TERM
SECOND ORDER
THIRD ORDER
EXPERIMENTAL DATA
STRESS
STRAIN
TIME (SEC.)
+ 450 PSI
+ 300 PSI
+ 150 PSI
- 150 PSI
- 300 PSI
- 450 PSI
+0.03
+0.01
-0.01
-0.02
0
600
1200
1800
3000
3600
4200

FIG. 24

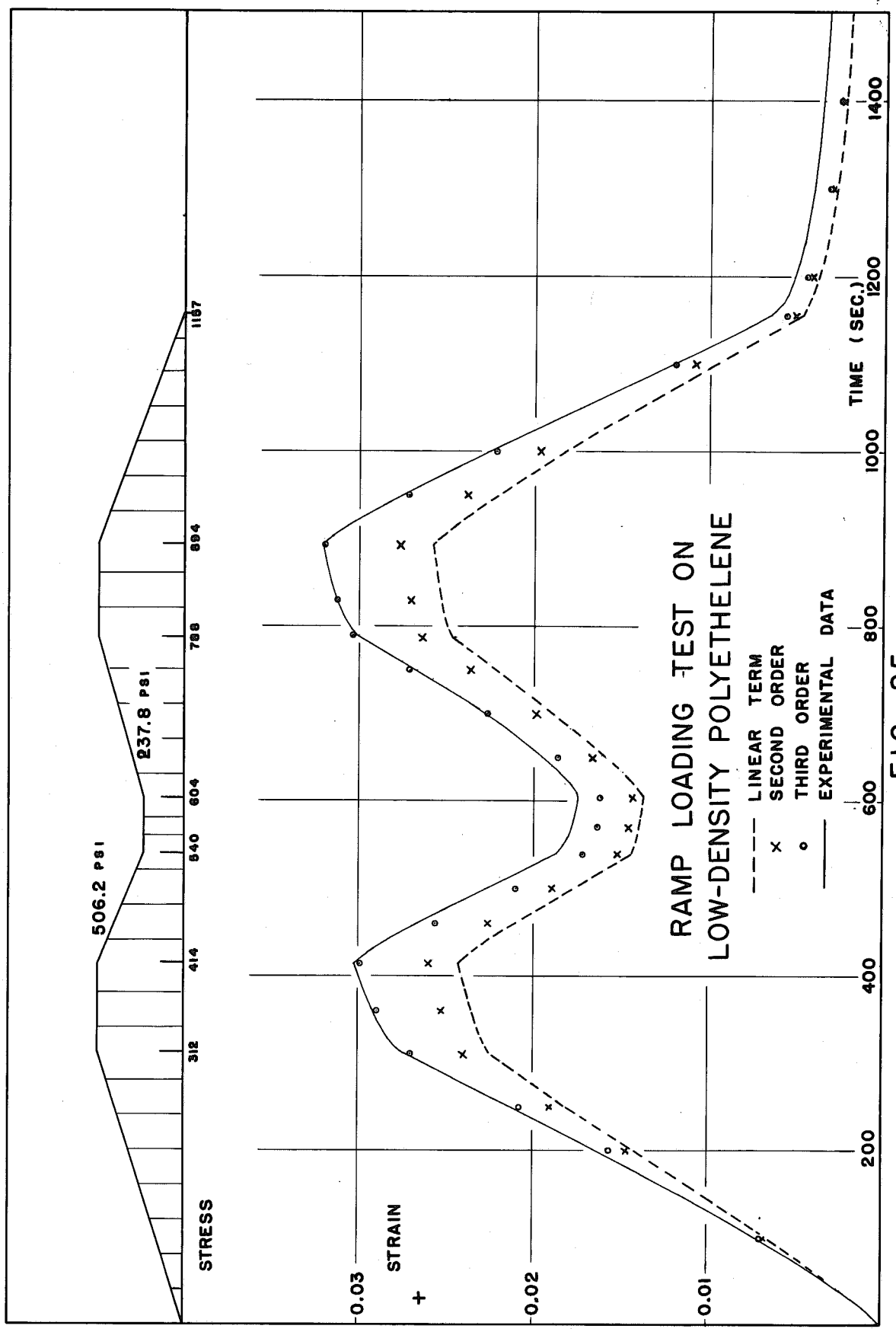
RAMP LOADING TEST ON
LOW-DENSITY POLYETHELENE
LINEAR TERM
SECOND ORDER
THIRD ORDER
EXPERIMENTAL DATA
STRAIN
+
0.03
0.02
0.01
TIME (SEC.)
200
400
600
800
1000
1200
1400
STRESS
506.2 PSI
237.8 PSI
312
414
540
604
788
894
1157

FIG. 25

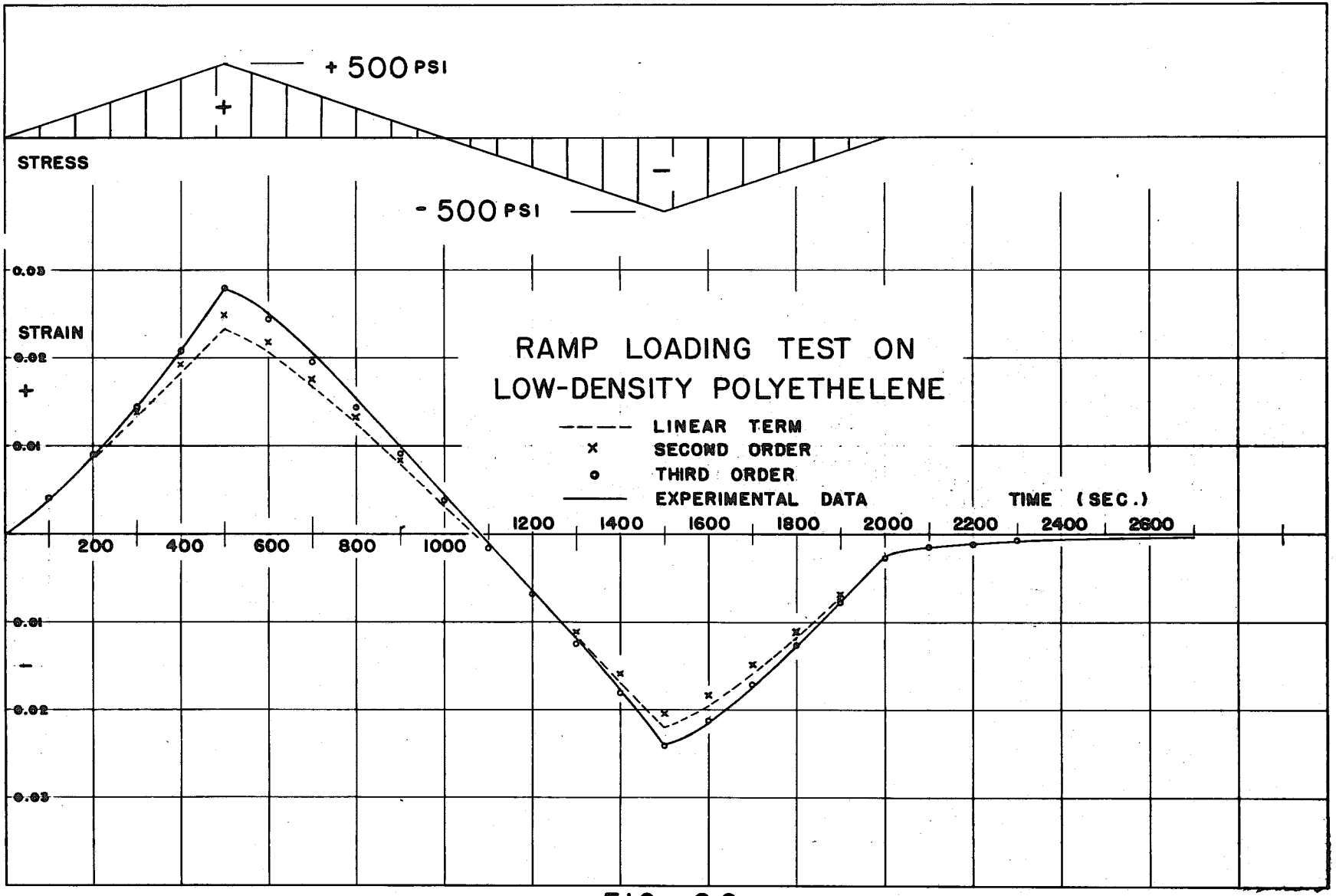
+ 500 PSI
STRESS
- 500 PSI
STRAIN
0.03
0.02
+
0.01
0.01
-
0.02
0.03
RAMP LOADING TEST ON
LOW-DENSITY POLYETHELENE
LINEAR TERM
SECOND ORDER
THIRD ORDER
EXPERIMENTAL DATA
TIME (SEC.)
200
400
600
800
1000
1200
1400
1600
1800
2000
2200
2400
2600

FIG. 26